QEX
A Forum for
Communications Experimenters

November / December 2023
Issue No. 341 | www.arrl.org

SP3L designs wide-band ground-independent wire antennas.

The EVENT HORIZON OF DX

TS-990S

Dual TFT Display & Dual Receiver HF/50 MHz Transceiver

The main receiver has an IP3 in the +40 dB class, and the sub-receiver is the already famous TS-590S receiver. Capable of receiving two signals at once, on different bands. 7-inch and 3.5-inch color TFT displays allow displaying of independent contents. Simplification of complex operations at a glance. Make no mistake, this is not a toy. Finally a serious tool is available for getting the very most from your hobby - of course it's a Kenwood.

- Covers the HF and 50 MHz bands.
- High-speed automatic antenna tuner.
- USB, Serial and LAN ports.
- Various PC applications (free software): ARCP-990 enabling PC control, ARHP-990 enabling remote control, and ARUA-10 USB audio driver.
- Clean 5 to 200 W transmit power through the 50 V FET final unit.
- Built-in RTTY and PSK.
- Three Analog Devices 32-bit floating-point arithmetic DSPs.
- DVI output for display by an external monitor (main screen display only).

KENWOOD

Customer Support: (310) 639-4200
Fax: (310) 537-8235

Scan with your phone to download TS-990S brochure.

www.kenwood.com/usa

ISO9001 Registered
JVCKENWOOD Corporation

ADS#15115

QEX

QEX (ISSN: 0886-8093) is published bimonthly in January, March, May, July, September, and November by the American Radio Relay League, 225 Main St., Newington, CT 06111-1400. Periodicals postage paid at Hartford, CT and at additional mailing offices.

POSTMASTER: Send address changes to: QEX, 225 Main St., Newington, CT 06111-1400 Issue No. 340

Publisher
American Radio Relay League

Kazimierz "Kai" Siwiak, KE4PT
Editor

Lori Weinberg, KB1EIB
Assistant Editor

Ray Mack, W5IFS
Contributing Editors

Production Department
Becky R. Schoenfeld, W1BXY
Director of Publications and Editorial

Jodi Morin, KA1JPA
Assistant Production Supervisor

David Pingree, N1NAS
Senior Technical Illustrator

Brian Washing
Technical Illustrator

Advertising Information
Janet L. Rocco, W1JLR
Business Services
860-594-0203 – Direct
800-243-7768 – ARRL
860-594-4285 – Fax

Circulation Department
Cathy Stepina
QEX Circulation

Offices
225 Main St., Newington, CT 06111-1400 USA
Telephone: 860-594-0200
Fax: 860-594-0259 (24-hour direct line)
Email: **qex@arrl.org**

Subscription rate for 6 print issues:
In the US: $29

US by First Class Mail: $40

International and Canada by Airmail: $35

ARRL members receive the digital edition of *QEX* as a member benefit.

In order to ensure prompt delivery, we ask that you periodically check the address information on your mailing label. If you find any inaccuracies, please contact the Circulation Department immediately. Thank you for your assistance.

November/December 2023

About the Cover

Jacek Pawlowski, SP3L, introduces designs that use closely spaced wires to achieve a wide-band antenna capable of spanning multiple ham bands. This end-fed antenna, named the LPi, has many interesting features. It is ground-independent and is very slim. If used as a vertically polarized antenna, it can be installed in places where a ground plane (GP) antenna does not fit because the GP requires space for its counterpoise. The LPi radiation pattern and gain are very close to that of a half-wave dipole. Ground proximity affects the antenna SWR performance in a very moderate way. It is possible to adjust the LPi bandwidth by changing its proportions. Its bandwidth can be large enough to cover two or, in some cases, even three neighboring ham bands. The LPi is easy to simulate using numerical electromagnetic code (NEC).

In This Issue:

Index of Advertisers

The American Radio Relay League

The American Radio Relay League, Inc., is a noncommercial association of radio amateurs, organized for the promotion of interest in Amateur Radio communication and experimentation, for the establishment of networks to provide communications in the event of disasters or other emergencies, for the advancement of the radio art and of the public welfare, for the representation of the radio amateur in legislative matters, and for the maintenance of fraternalism and a high standard of conduct.

ARRL is an incorporated association without capital stock chartered under the laws of the state of Connecticut, and is an exempt organization under Section 501(c)(3) of the Internal Revenue Code of 1986. Its affairs are governed by a Board of Directors, whose voting members are elected every three years by the general membership. The officers are elected or appointed by the Directors. The League is noncommercial, and no one who could gain financially from the shaping of its affairs is eligible for membership on its Board.

"Of, by, and for the radio amateur," ARRL numbers within its ranks the vast majority of active amateurs in the nation and has a proud history of achievement as the standard-bearer in amateur affairs.

A *bona fide* interest in Amateur Radio is the only essential qualification of membership; an Amateur Radio license is not a prerequisite, although full voting membership is granted only to licensed amateurs in the US.

Membership inquiries and general correspondence should be addressed to the administrative headquarters:

ARRL
225 Main St.
Newington, CT 06111 USA
Telephone: 860-594-0200
FAX: 860-594-0259 (24-hour direct line)

Officers

President: Rick Roderick, K5UR
P.O. Box 1463, Little Rock, AR 72203

The purpose of *QEX* is to:

1) provide a medium for the exchange of ideas and information among Amateur Radio experimenters,

2) document advanced technical work in the Amateur Radio field, and

3) support efforts to advance the state of the Amateur Radio art.

All correspondence concerning *QEX* should be addressed to the American Radio Relay League, 225 Main St., Newington, CT 06111 USA. Envelopes containing manuscripts and letters for publication in *QEX* should be marked Editor, *QEX*.

Both theoretical and practical technical articles are welcomed. Manuscripts should be submitted in word-processor format, if possible. We can redraw any figures as long as their content is clear. Photos should be glossy, color or black-and-white prints of at least the size they are to appear in *QEX* or high-resolution digital images (300 dots per inch or higher at the printed size). Further information for authors can be found on the Web at **www.arrl.org/qex/** or by e-mail to **qex@arrl.org**.

Any opinions expressed in *QEX* are those of the authors, not necessarily those of the Editor or the League. While we strive to ensure all material is technically correct, authors are expected to defend their own assertions. Products mentioned are included for your information only; no endorsement is implied. Readers are cautioned to verify the availability of products before sending money to vendors.

Kazimierz "Kai" Siwiak, KE4PT

Perspectives

Earth, Water, Air and Fire

The four classical elements embodied in their destructive form as earthquakes, floods, cyclones and wildfires have inundated the news as they wreak deadly havoc around the globe. We can add the aether as a fifth classical element that we interpret as radio waves and their propagation. Of the five elements, the manifestation of aether as radio wave propagation is the beneficial element, and the one to which we can directly relate.

One of the main tenets of amateur radio is that we help by providing disaster area communications at the front line for those in troubled areas. Specialized communicator knowledge and skills among radio amateurs about antennas, radios, modulations, and the standardization of communications protocols among emergency preparedness organization is widely recognized. This is a shout-out to all radio amateurs, and especially to *QEX* members, who have rendered their invaluable assistance in the emergency spots around the world.

QEX is a journal for communications experimenters. It is a disseminator of radio technologies and their advances. But in a larger sense it is a forum for communicators. Among the ranks of experimenters, authors and readers are a cadre of emergency radio communications volunteers, whom we salute.

In This Issue:

- Michael Reinhold, HB9BEP, and Martin Klaper, HB9ARK, use FT8 contacts to study ionospheric radio propagation.
- Jacek Pawlowski, SP3L, designs a wide-band end-fed wire antenna.
- Marcel De Canck, ON5AU, explains the use of *EZNEC Pro+ v.7.0* and *AutoEZ*.
- Dennis G. Sweeney, WA4LPR, describes phase noise measurements.
- Eric P. Nichols, KL7AJ, in his Essay #19 discusses the Smith Chart.

Writing for *QEX*

Please continue to send in full-length *QEX* articles, or share a **Technical Note** of several hundred words in length plus a figure or two. *QEX* is edited by Kazimierz "Kai" Siwiak, KE4PT, (**ksiwiak@arrl.org**) and is published bimonthly. *QEX* is a forum for the free exchange of ideas among communications experimenters. All members can access digital editions of all four ARRL magazines: *QST*, *OTA, QEX*, and *NCJ* as a member benefit. The *QEX printed edition* is available at an annual subscription rate (6 issues per year) for members and non-members, see **www.arrl.org/qex**.

Would you like to write for *QEX*? We pay $50 per published page for full articles and *QEX* Technical Notes. Get more information and an Author Guide at **www.arrl.org/qex-author-guide**. If you prefer postal mail, send a business-size self-addressed, stamped (US postage) envelope to: *QEX* Author Guide, c/o Maty Weinberg, ARRL, 225 Main St., Newington, CT 06111.

Very kindest regards,
Kazimierz "Kai" Siwiak, KE4PT
QEX Editor

Marcel De Canck, ON5AU
Schoolstraat 8, B8880, Rollegem-Kapelle, Belgium | **on5au.43@gmail.com**

EZNEC Pro+ v.7.0 and *AutoEZ* – Part 1

EZNEC with *AutoEZ* form a powerful electromagnetic analysis combination.

Now that *EZNEC Pro+ v.7.0* is available for free, it cannot be a budget limit to start with antenna modeling. Some hams will only use it to model the antennas they use or are planning to use. Others interested in the antenna properties, radiation, and general behavior can now thoroughly investigate and explore. Sure, it takes a while to get the hang, but then you will have a great time.

EZNEC History

In the early 1980s, the first antenna modeling program, *MININEC*, for small desktop personal computers became available. At about the same time, the Lawrence Livermore National Laboratory developed *NEC* under the leadership of Jerry Burke. The most common and public domain version, *NEC-2*, was developed in 1981. This version has evolved into *NEC-3* (1985), *NEC-4* (1992), *NEC-4.2* (2011), and the latest version, *NEC-5* (2019).

In 1991 and 1992, Roy Lewallen, W7EL, and Brian Beezley, K6STI, introduced advanced versions of *MININEC*, such as *ELNEC*, *MN*, and *AO*, which included better user interfaces and graphic displays.

In 1995 *EZNEC v.1.0* became available, and *v. 2.0* in 1997. Both were DOS programs. Instead of *ELNEC* based on the *MININEC* calculation engine, *EZNEC* uses the *NEC-2* engine, which was released into the public domain as an open source.

EZNEC v.3.0 was the first *Windows* version and was released in 2000. At the same time, the *Pro* versions became available, in either *NEC-2* or *NEC-4*. You must first obtain a license from the Lawrence Livermore National Laboratory for the latter. More versions followed as *v.4.0* in 2005, then *v.5.0* in 2008, after that *v6.0* in 2015, and nowadays, *v.7.0* in 2022.

In the same period of *EZNEC v.3*, Nittany-Scientific launched *NEC-Win-Plus* and *Pro*. At that time, of the available *NEC-2* programs, perhaps *NEC-Win-Plus* offers the most versatile modeling system in this way. For example, the use of variables and equations. It uses a spreadsheet input screen and allows users to see alternative spreadsheet views. A) the numbers and equations used to set the values of variables. B) the values that result from those equations. C) the assignment of variables to the *X*, *Y*, and *Z* coordinates of the model structure. D) the physical values of the *X*, *Y*, and *Z* coordinates that result from the preceding steps.

The lack of these spreadsheet options were a short coming in *EZNEC*. However, Dan Maguire, AC6LA, wanted to use *EZNEC* similarly, so he created an *Excel* application using macros to allow these options. His first *Excel* application became available in 2003, named *MultiNEC*. After that, Dan added more options and features. The resulting application became available as *AutoEZ* (Automated use of *EZNEC*) in 2013.

Modeling with *AutoEZ*

AutoEZ is an *Excel* application that works in conjunction with the *EZNEC v. 5.0*, *v. 6.0*, and *v. 7.0* antenna modeling programs by Roy Lewallen. *AutoEZ* requires *Excel 97* or later. *AutoEZ* will not operate correctly with other spreadsheet software such as *Open Office Calc*, *Quattro Pro*, *Microsoft Works*, *Excel Starter*, or versions of *Excel* earlier than *Excel 97*. None of these other spreadsheet programs fully support the macros used by *AutoEZ*.

The *AutoEZ* **[1]** application can make multiple simulation runs of an antenna model while automatically changing one or more aspects of the model between runs. The model can be automatically changed between runs in several ways. The simplest is to use a different frequency for each test case, equivalent to a standard frequency sweep. You can also specify that one or more wires in the model are to be rotated, moved, made longer or shorter, scaled, or have a different segmentation level between runs. You can change the parameters of sources, loads, transmission lines, stubs, transformers, and **L** networks. Such as the position of a source along a wire, the $R \pm jX$ or *RLC* values for a load, transmission line (stub) lengths, the transformer ratio, or the capacitance and inductance of the **L** network.

AutoEZ contains complete modeling by equation facility. You can create the model using *Excel* spreadsheets and then instruct the program to change the geometry or other aspect of the model

in any way that can be specified using *Excel* formulas. A scratchpad is available for any needed pre-calculations or for giving pieces of information about the model. All these changes may be made automatically without requiring manual intervention between simulation runs.

Finally, with *AutoEZ*, it is easy to trim the model on a design frequency or optimize the model to a target impedance resistance, reactance, SWR, gain, front-to-back ratio, and front-to-rear ratio for a good enough value.

The simulation results are available in tabular or various graphical plot formats. These include three standard rectangular plots, far and near field plots, impedance $R \pm jX$, SWR, gain, current, and user's definable types. You can combine most graphical plots by using the snapshots option.

I recommend installing *EZNEC Pro+ v.7.0* and the *AutoEZ* free demo. This demo version is limited to using only 30 segments but is not a limitation for the first few model examples. This free version allows you to explore all the *AutoEZ* features and options. This combination gives you a no-cost way to see if *AutoEZ* is right for you.

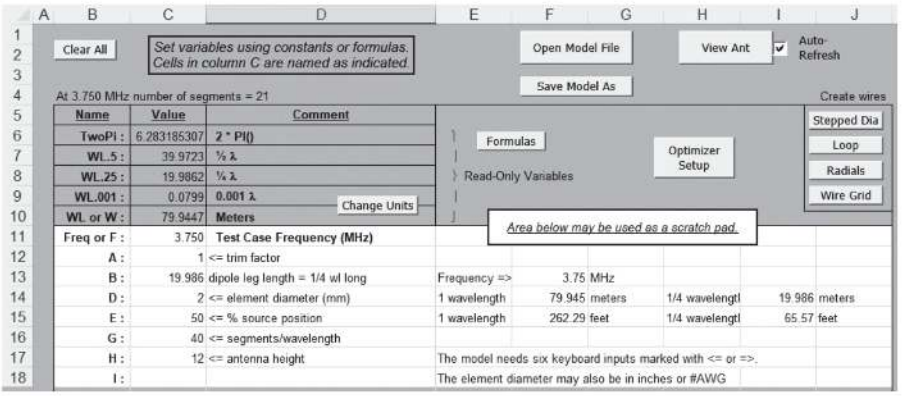

Figure 1a — The Variables sheet. [dipole-1a.weq] [dipole-1a.ez].

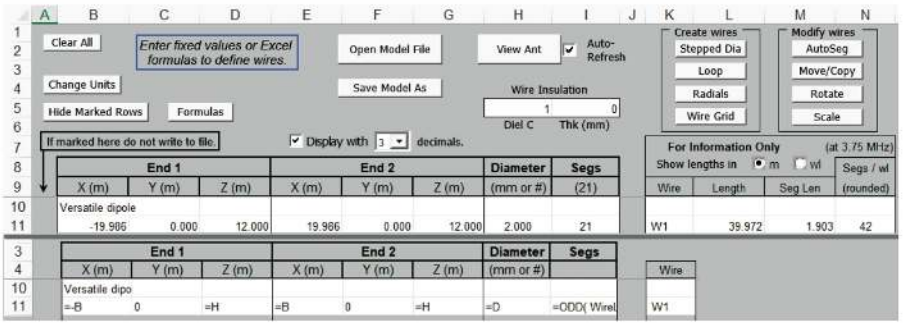

Figure 1b — At the top is the Wires sheet, and at the bottom is the Wires > Formulas > TempEdit sheet.

Dipole

You can define an antenna model either by building it from scratch or opening an existing model. Knowing elementary *Excel* usage is a plus point. Let's start by designing a simple dipole antenna example to demonstrate a model's buildup and lets you get experience and knowledge, and become familiar with using *AutoEZ*. Although I have an 80-meter antenna in mind, I want to make the model versatile to change the frequency band easily. It must also be easy to trim the antenna to become resonant on the design frequency, and to change the height. The possibility of putting the source off-center and performing an easy convergence test is also desirable. Depending on where you live, you shall mostly use either imperial units or metric units. So, specify the units you usually use by the option button **Change Units** in the *Variables* or *Wires* worksheet.

Variables

This sheet **(Figure 1a)** defines the variables that may be used in *Excel* formulas. The variables may also be set equal to numeric constants (as with **A, D, E, G**, and **H** or may be defined in terms of other variables and intermediate *Excel* formulas as used in the scratchpad calculations cell **I14 =ROUND(F14/4;3)**. By changing the values for variables on the *Variables* sheet, you (or *AutoEZ* as with variable **A**, see later) can change the geometry of the wires in your model and, or change the parameters that control the sources, loads, transmission lines, transformers, and **L** networks.

Please note that I used the semicolon (;) punctuation to mark the rounded decimal places. However, it has to be a comma (,) in countries utilizing the decimal radix. So in the US and the UK, the function would be **=ROUND(F14/4,3)**. Using a model where the semicolon is used, *Excel* will automatically replace it with a comma and *visa versa*.

To start with the model, open the *Variables* sheet and define variable **A** with a default trim factor value of 1. We know that the electrical length of a dipole at resonance is shorter than the physical half wavelength depending on the end effect, element diameter, antenna height, ground quality, and surroundings. With *AutoEZ*, we have the option to use this factor to bring the dipole automatically to resonance on a given frequency.

Next, specify the design resonance frequency in the scratchpad area (3.75 MHz) in cell **F13**. Now we can calculate the one wavelength either in meters or in feet. For meters, we use the formula **=ROUND(299.792458/F13*A;3)** in cell F14, and **=ROUND(983.571/F13*A;2)** in cell **F15** for feet. The formula is *(speed of light)/frequency.* However, I added the multiply trim factor variable **A**. To define the dipole wire coordinates, we need the 1/4 wavelength, which we calculate in cells **I13** and **I14** with the formulas **=ROUND(F14/4;3)** or **=ROUND(F15/4;2)**. In cell **C13** (variable **B**), we put the equation **=I14** or **=I15** (depending on the units you use). This cell refers to the trimmed dipole leg length. Variables **D, E, G**, and **H** are self-explanatory.

Wires

This worksheet **(Figure 1b)** is very similar to the Wires window of *EZNEC*, except that you may use *Excel* formulas and numeric constants as well for the *XYZ* coordinates, wire diam-

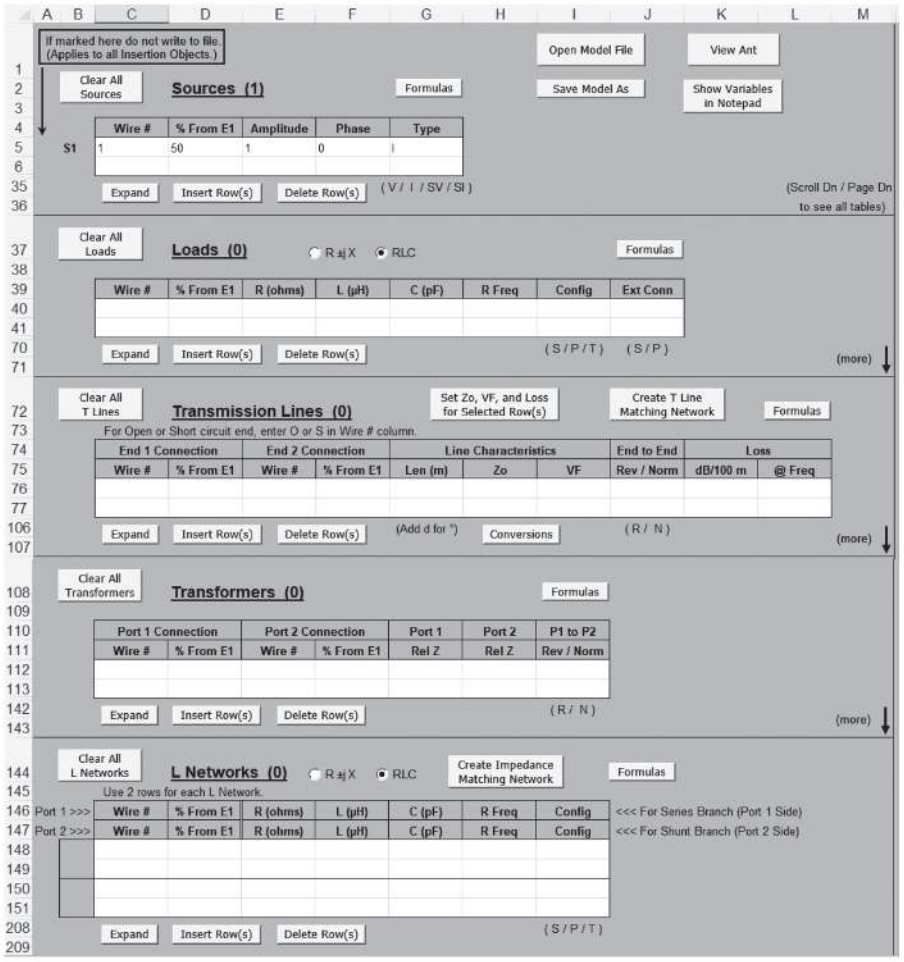

Figure 1c — The Insr Objs sheet has five insert object dialogs: Sources, Loads, Transmission Lines, Transformers, and L Networks.

Insr Objs

This sheet (**Figure 1c**) defines the **Sources**, **Loads**, **Transmission Lines**, **Transformers**, and **L** Networks. The five sections of this sheet are again very similar to the corresponding windows of *EZNEC*. Again you may use variables and *Excel* formulas as well as numeric constants. However, A*utoEZ* has additional Transmission Lines and **L** Networks features. The former has two extras: **Set Zo, VF, and Loss for Selected Row(s)** and **Create T Line Matching Network**, and later: **Create Impedance Matching Network**. These extras are powerful and versatile additions and will be handled later.

For our dipole model, we only need to define a source (**Figure 1c**). Remember, for the **% From E1** cell, we use the variable **=E** instead of a numerical constant. Important note: you must define at least one source. *EZNEC* will warn you if you do not. You cannot run a model or do any calculations for a model without a source. Our model is now complete and ready to perform calculations.

Calculate

This sheet (**Figure 2a**) performs calculation results in various numerical data, graphical displays, and plots. You must define at least one frequency whereon to calculate. To start, I keep it simple and do a calculation on the design frequency. Before starting calculations, we must specify a **Ground Type**, the **Wire Loss**, and a **Plot/Slice**. You can begin the calculations by clicking the **Calculate All Rows** button.

The calculation results are impedance = 67.87 + j74.41 Ω, SWR(50) = 3.435, and a gain of 6.33 dBi at the elevation angle of 90°. These items are written on the right side of the Calculate sheet. Because the reactance is a positive value, we know the physical dipole length is too long. If you'd like to know on what frequency this dipole resonates, click the **Resonate on Selected Cell** button. The result is 3.6 MHz, with impedance = 58.39 + j0.00 Ω, SWR(50) = 1.168, and a gain of 6.24 dBi. However, we want to trim the dipole length on the design frequency by using the variable **A**.

Reset the frequency again to 3.75 MHz. Define this variable A in cell C10 and value 1 in cell C11, the **Variable Name** and values setup area. Select cell C11 with the value 1 and click the Resonate on Selected Cell button. It takes a few automatic calculations, and the resonant result becomes an impedance = 60.13 – j0.05 Ω, SWR(50) = 1.203, and a gain of 6.28 dBi. The variable **A** (the trim factor) became 0.9598303, which is very close to the recommended textbook value for a low-band dipole.

AutoEZ does not just try random values to answer such a trim question. Three test cases are calculated, and the three sets of results are used to perform a second-order polynomial regression

eter, and the number of segments. Although not obvious in the figure, the *XYZ* coordinates, element diameter, and the number of segments of the model used for illustration purposes were not entered as numerical constants. Instead, they were defined in terms of *Excel* formulas or equations using variables with values set on another worksheet.

To define the dipole coordinates and parameters, open the *Wires* sheet and set the wire **End 1**, **End 2**, and **diameter** cells as shown at the bottom of **Figure 1b**. Note that the *X*-axis **End 1** is negative, and **End 2** is positive. Putting the center of wires at the *X*–0 position is good practice. Thus a wire tip-end left and the other right. The formula in the **Segs** cell is not manually set. To define the number of segments, we use the **AutoSeg** option available at the top right corner; modify wires buttons of the *Wires* sheet. In the **AutoSeg Wires** dialog box, define the variable **G**, check **Segments** per wavelength, ensure an odd number of segments, and **Apply** it to *All Wires*.

Note that the odd number of segments is needed with *NEC-2* and *NEC-4* to ensure the source (or any *Insert Object*) is at the exact center of the wire. With *NEC-5*, this is not required because inserting objects happens at a segment's connection point, but the wire must have an even number of segments.

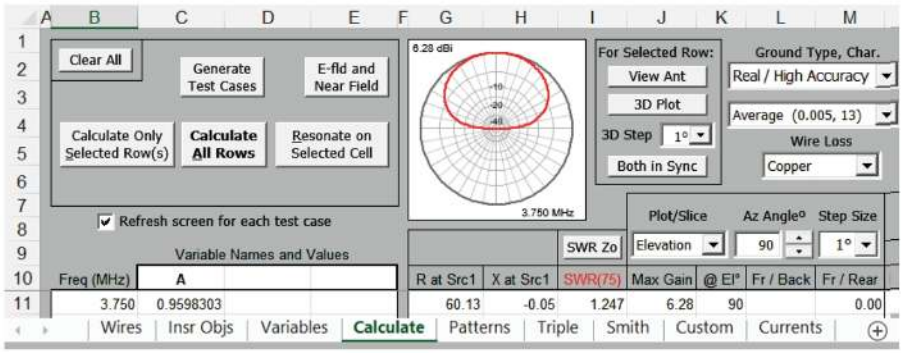

Figure 2a — The Calculate sheet for the dipole calculations upon one frequency. [dipole-1b.weq], [dipole-1b.ez].

Freq (MHz)	A	R at Src1	X at Src1	SWR(75)	Max Gain	@ El°	Fr / Back	Fr / Rear
3.500		47.18	-119.37	6.081	6.12	90		0.00
3.550		49.54	-95.35	4.394	6.16	90		0.00
3.600		52.01	-71.44	3.124	6.19	90		0.00
3.650		54.59	-47.60	2.201	6.22	90		0.00
3.700		57.30	-23.83	1.567	6.25	90		0.00
3.750	0.9598303	60.13	-0.05	1.247	6.28	90		0.00
3.800		63.11	23.66	1.466	6.31	90		0.00
3.850		66.24	47.36	1.956	6.33	90		0.00
3.900		69.51	71.07	2.588	6.36	90		0.00
3.950		72.94	94.82	3.345	6.38	90		0.00
4.000		76.53	118.62	4.215	6.40	90		0.00

Figure 2b — The Calculate sheet for the dipole calculations upon a frequency range. [dipole-2.weq], [dipole-2.ez].

Freq (MHz)	H	A	R at Src1	X at Src1	SWR(75)	Max Gain	@ El°	Fr / Back	Fr / Rear
3.750	7.5		47.35	-6.37	1.603	4.76	90		0.00
3.750	10		53.54	-2.13	1.403	5.86	90		0.00
3.750	12.5	0.9597226	61.85	-0.03	1.213	6.34	90		0.00
3.750	15		70.44	-0.73	1.066	6.46	90		0.00
3.750	17.5		78.05	-4.03	1.068	6.33	90		0.00
3.750	20		83.80	-9.34	1.176	6.15	62		0.00
3.750	22.5		87.22	-15.82	1.280	6.07	53		0.00
3.750	25		88.17	-22.59	1.377	6.09	46		0.00

Figure 2c — The Calculate sheet with the setup to calculate on a range of heights. [dipole-3.weq], [dipole-3.ez].

analysis. The *Y*-intercept of this analysis is used as the "best guess" for the second set of these test cases. This process is repeated until the antenna resonance point is found, with automatic checkpoints to allow for manual intervention in case the process is not converging.

Knowing the bandwidth for some antennas, particularly for the lower frequency bands, might be necessary. So a frequency sweep over the entire bandwidth is required. We can define the start frequency, stop frequencies, and step size with the **Generate Test Cases** option at the left-top of the *Calculate* sheet. Do not forget to trim the dipole before performing the frequency sweep, see **Figure 2b**.

Suppose you want to know the results when the dipole is installed at various heights (**Figure 2c**). We must now define variable **H** in cell **C10** and specify in column **C** a range of heights, for example, from 7.5 meters to 25 meters in steps of 2.5 meters. You can do this by manual keyboard numerical constants inputs, but using the *Excel* fill handle is much more time-saving and handier. I will explain for those hams with little *Excel* experience. Enter **7.5** in cell **C11** and **10** in cell **C12**. Select both cells, and you will see a little square point in the lower-right corner (the *Excel* fill handle). Point now the *Excel* cursor close to that square point, and when the cursor changes to a plus sign (+), press and hold the left mouse button and drag down six cells along the column, thus dragging downward until you reach the value 25. Next, select cell **B11** with the frequency of 3.75 MHz and repeat the dragging down action along the **B** column until you get to row 18. Of course, by using variable **A**, we can trim for resonance at any of the heights.

The subsequent research is moving the source position (**Figure 2d**). We must now define variable **E** in cell **C10** and specify in column **C** a range of percentages from Wire End 1. For example, from 5% to 50% meters in steps of 5%. Again, using the *Excel* fill handle is handy.

First, perform a **Resonate on Selected Cell** using the variable **A** in cell **D20.** After that, run a **Calculate All Rows**. From the results, we may conclude that the source position significantly impacts the impedance. The closer the source is to the element tip, the higher the resistance and reactance. However, off-center-fed can be a reason for a shorter transmission line length to the equipment. In this case, a transformer balun is necessary. For example, use a 2:1 balun with the source at 25%. An eye-catcher is that the source position does not influence the gain and the radiation properties stay the same.

For an 80 or 40-meter dipole, we use wire. However, we might use an aluminum tube for the high HF bands to allow rotation. **Figure 2e.** Use the variable **D**, specifying the element diameter. Resonate the dipole again using variable **A**, one with a diameter of 1 mm and one with a diameter of 30 mm. The results reveal negligible changes for the impedance, gain, and maximum gain elevation angle. But we notice a significantly different dipole length. With a 1 mm wire, the dipole length is 10.254 meters. When using a 30 mm tube, the dipole length becomes 10.104 meters, thus 0.15 meters (15 cm) shorter.

Note that all the calculations are done using average ground. Using another ground type will result in different values.

Besides numerical data results, *AutoEZ* and *EZNEC* can project the results in graphical charts. Patterns, Triple, Smith,

		Variable Names and Values				SWR Zo	Elevation	90	1°	
10	Freq (MHz)	E	A		R at Src1	X at Src1	SWR(75)	Max Gain	@ El°	Fr / Back	Fr / Rear
11	3.750	5			913.65	-304.24	13.541	6.27	90		0.00
12	3.750	10			388.51	-67.78	5.344	6.28	90		0.00
13	3.750	15			219.64	-22.70	2.964	6.28	90		0.00
14	3.750	20			145.94	-9.30	1.957	6.28	90		0.00
15	3.750	25			107.85	-4.23	1.442	6.28	90		0.00
16	3.750	30			86.16	-1.99	1.151	6.28	90		0.00
17	3.750	35			73.20	-0.92	1.028	6.28	90		0.00
18	3.750	40			65.52	-0.38	1.145	6.28	90		0.00
19	3.750	45			61.42	-0.12	1.221	6.28	90		0.00
20	3.750	50	0.9598303		60.13	-0.05	1.247	6.28	90		0.00

Figure 2d — The Calculate sheet with the setup to calculate on a range of source positions. [dipole-4.weq], [dipole-4.ez].

		Variable Names and Values				SWR Zo	Elevation	90	1°	
10	Freq (MHz)	A	D		R at Src1	X at Src1	SWR(75)	Max Gain	@ El°	Fr / Back	Fr / Rear
11	14.175	0.9734712	1		66.13	-0.17	1.134	7.62	24		0.00
12	14.175	0.9555414	30		63.61	-0.07	1.179	7.78	24		0.00

Figure 2e — The Calculate sheet with the setup to calculate different element diameters. [dipole-5.weq], [dipole-5.ez].

Custom, and Current chart sheets are available with *AutoEZ*. The *EZNEC* **View Ant** window option is available in the Wires, Insr Objs, Variables, Calculate, and Patterns sheets. So you can have a quick view of how your model evolves. The *EZNEC* **3D Plot** option is available in the *Calculate* and *Patterns* sheets.

Triple

This sheet **(Figure 3a)** contains three standard rectangular plots. 1) *R* and *X*, 2) SWR, and 3) Max Gain, Front/Back ratio Front/Rear ratio. The Front/Back ratio is calculated for azimuth patterns only but is displayed for elevation patterns only in free space. The horizontal scale for all three plots is the same and is automatically set by *AutoEZ*. It will typically be whatever the changing value was between the test cases, such as frequency, antenna height, % source position, etc. If no variables were changed between test cases on the Calculate sheet, and instead, the frequency was changed, the horizontal scale would be frequency.

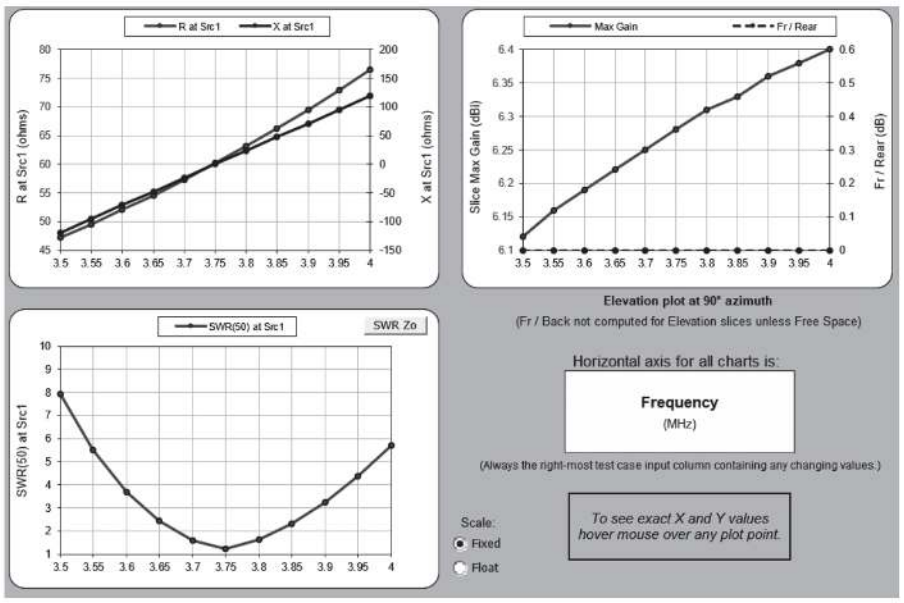

Figure 3a — The Triple sheet shows three standard rectangular plots.

Patterns

After any test cases run (**Figure 3b**), you may switch to the *Patterns* sheet. Initially, this sheet will show the elevation or the azimuth plot for the first test case, corresponding to **row 11** on the *Calculate* sheet. You may use the spinner for cycling through the other test cases. The scrollbar positions the marker to a particular elevation or azimuth angle and see detailed information concerning that point. The plot can be scaled with the *ARRL* modified log scale (the same as the default for *EZNEC* polar plots) and a linear scale. The *Patterns* sheet also provides a rectangular plot; you can swap the plots.

With the **Snapshot** button, it is easy to capture and freeze a plot trace so that you may compare that trace to others from the same set of test cases or generated with different parameters. For example, you could request an elevation plot, take a snapshot, then request an azimuth plot and show the results superimposed on the same chart. The snapshot trace will remain in place until it is manually erased or hidden and auto-scale with the primary trace. Or you can compare several snapshot elevation plots of different antenna heights and superimpose them into one chart.

Custom

This sheet (**Figure 3c**) can be used to build a completely free-form rectangular plot. Both the horizontal (*X*) and the vertical (*Y*) scales may be set to your choosing, picking from Frequency any variables that were put on the *Calculate* sheet and any data items extracted from the simulation output data files. **Figure 3c** shows an example that plots the maximum gain versus the antenna height.

The **Snapshot** button works exactly like the one on the *Patterns* sheet. However, the possibility of taking four snapshots might be fascinating to compare a maximum of five plots. You can capture any trace and compare it against any other trace. For example, you could plot SWR(50) versus frequency, take a snapshot, then change the SWR reference to 75 Ω and compare the traces. (Note that the SWR reference base may be changed at any time without the need to recalculate all the test case results). Or you could plot gain versus some other parameter, take a snapshot, change the model's geometry, recalculate the test case, then compare the old gain curve to the new one. Nineteen

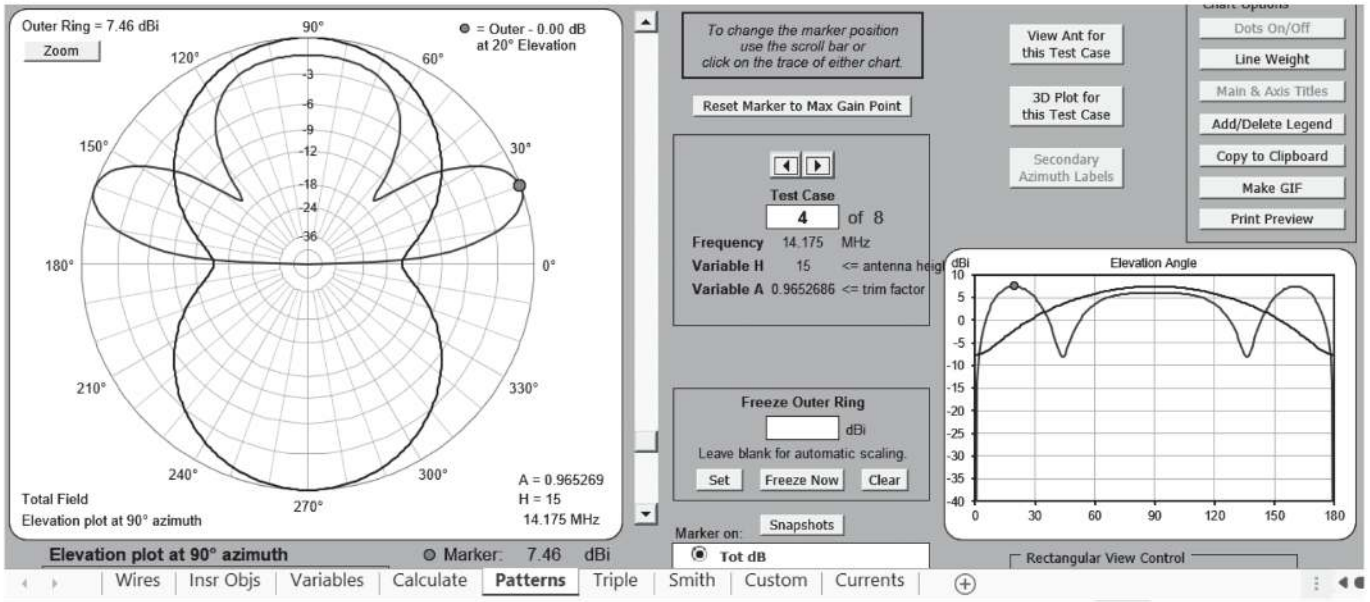

Figure 3b — The Patterns sheet shows the elevation plot superimposed with the azimuth plot using the snapshot option.

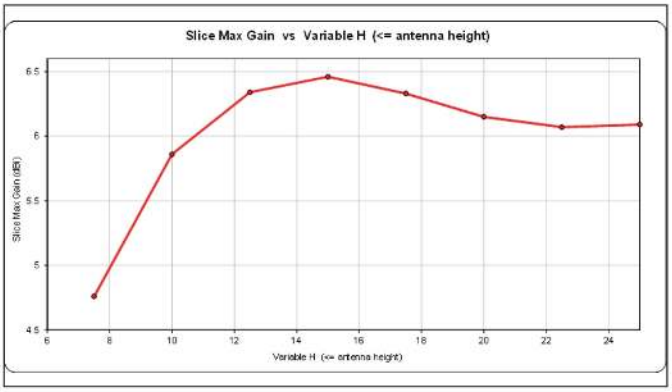

Figure 3c — The Custom plot of the Maximum Gain (dBi) vs. the antenna height (variable H).

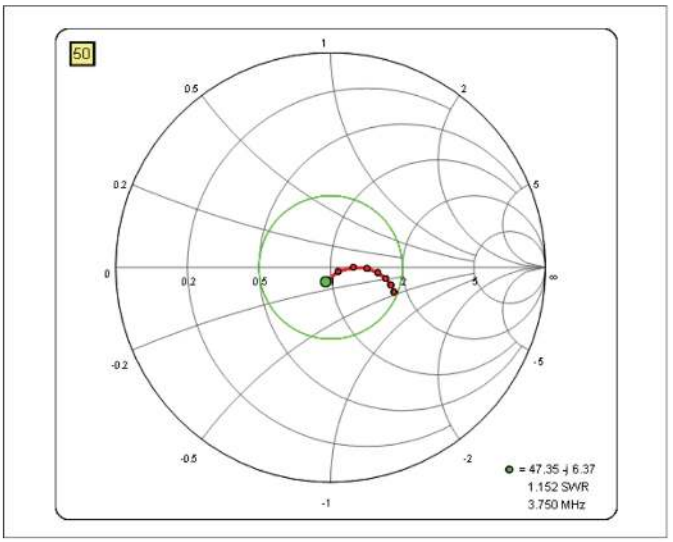

Figure 3d — The Smith sheet shows the SWR at 3.75 MHz and with the antenna at various heights.

parameters are available to combine the *X*- and *Y*-axis plot parameters.

Smith

The SWR can also be projected on a Smith chart (**Figure 3d**). The illustration shows the SWR at 3.75 MHz with the antenna at various heights. Such a Smith chart gives you an idea about the bandwidth quickly.

V and L Shape Dipoles

Let's use another dipole model with trigonometric functions to calculate various **V** and **L** shaped antennas. **Figure 4a** shows the Variables sheet of this model. Compared to the previous straight dipoles, we have some additional variables. **D** defines the angle when we want the antenna sloped. **E** sets the length of one segment of a very short source wire having only three segments. We attach the two antenna arms to the source wire ends. We set the angles of the left- and right-side elements with the variables **H** and **I**.

At the scratchpad area (cell **G15**), we calculate again the trimmed to resonance half-wavelength antenna length. This length includes the short source wire. So, to obtain the antenna rotatable element length, we must subtract the 1.5-segment length of this source wire. In cell **G16**, we calculate this element length with the formula **=G15/2-1.5*E**, where **G15/2** is the trimmed quarter wavelength and **–1.5*E** is the half source wire length to be subtracted from the trimmed quarter wavelength.

Let's now consider the coordinates of the wires (**Figure 4b**). The *X*-axis cell **B11** gets the formula **=–(1.5*E+B*SIN(RADIANS(H)))**, where **B** is the rotatable antenna arm length, and **H** is the left-side element angle. Cell **E13** gets the formula **=(1.5*E+B*SIN(RADIANS(I)))**, where **I** is the right-side element angle. Notice the minus sign in front of the formula in cell **B11**.

The *X*-axis cells **B12** and **E11** get the formula **=–1.5*E,** and

11	Freq or F :	3.750	Test Case Frequency (MHz)		Area below may be used as a scratch pad.		
12	A :	0.9692361	<= Trim factor				
13	B :	19.334	Rotatable antenna arm length		Set Freq =>	3.75 MHz	
14	D :	45	<= Antenna slope angle (deg)		Calculator	Meter	Feet
15	E :	0.025	<= Minimum segment length source wire		Half-wave:	38.743	127.11
16	G :	20	<= Height source wire		Rotatable arm length	19.334	63.43
17	H :	60	<= Left-side arm angle (deg)		Note: angle is between arm and perpendicular line.		
18	I :	60	<= Right-side arm angle (deg)		When both angles are 90° we have a horizontal conventional dipole.		
19	J :	40	<= segments per wavelength		With angles 60° we have an inverted Vee with an apex angle of 120°.		
20	K :	2	<= element diameter (mm)		With 45° an apex angle of 90°, etc.		
21	L :				With an angle greater than 90° we rotate the arm upward.		
22	M :				Not only an inverted Vee model is possible but also a diversity of V- and L-shaped		
23	N :				antennas.		

Figure 4a — The Variables sheet for the V or L shaped models. [inverted-1.weq] [inverted-1.ez].

	A	B	C	D	E	F	G	H	I	J	K	L
8		End 1			End 2			Diameter	Segs		Show lengths in	
9		X (m)	Y (m)	Z (m)	X (m)	Y (m)	Z (m)	(mm or #)	(23)		Wire	Length
10		Inverted Vee										
11		-16.7812	0.0000	10.3330	-0.0375	0.0000	20.0000	2.0000	10		W1	19.3340
12		-0.0375	0.0000	20.0000	0.0375	0.0000	20.0000	2.0000	3		W2	0.0750
13		0.0375	0.0000	20.0000	16.7812	0.0000	10.3330	2.0000	10		W3	19.3340

Figure 4b — The Rotate Wires dialog box.

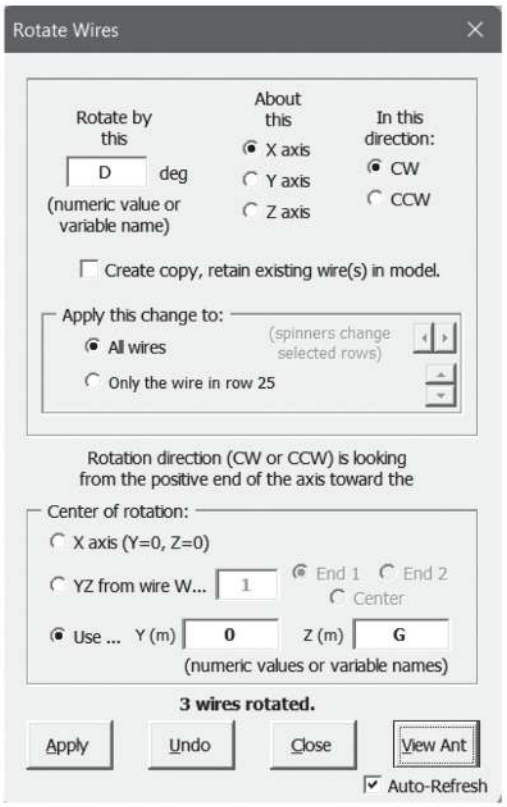

Figure 4c — The Wires sheet for the V or L shaped models.

		End 1			End 2			Diameter	Segs	Show le
9		X (m)	Y (m)	Z (m)	X (m)	Y (m)	Z (m)	(mm or #)	(23)	Wire
10	rx	Inverted Vee								
11	rx	-16.8120	0.0000	10.3153	-0.0375	0.0000	20.0000	2.0000	10	
12	rx	-0.0375	0.0000	20.0000	0.0375	0.0000	20.0000	2.0000	3	
13	rx	0.0375	0.0000	20.0000	16.8120	0.0000	10.3153	2.0000	10	
14	rx	Note: W1 and W3 may be defined as odd or even segments, nopreference.								
15	rx	However, W2 must be defined having 3 segments, see text.								
16		Inverted Vee								
17		-16.8120	-6.8482	13.1518	-0.0375	0.0000	20.0000	2.0000	10	W1
18		-0.0375	0.0000	20.0000	0.0375	0.0000	20.0000	2.0000	3	W2
19		0.0375	0.0000	20.0000	16.8120	-6.8482	13.1518	2.0000	10	W3

Figure 4d — The Wires sheet after the Rotate Wires. [inverted-2.weq], [inverted-2.ez].

cells **B13** and **E12** get the formula **=1.5*E**, where **E** is the minimum segment length of the source wire, and cells **B12** and **E11** are again negative values. Why **1.5*E**? The source wire is three segments long; thus, the ends of this wire are 1.5 segment lengths away from the wire center.

The *Z*-axis cell **D11** gets the formula **=G-B*COS(RADIANS(H))**, where **G** is the height of the source wire, **B** is the rotatable antenna arm length, and **H** is the left-side element angle. Cell **G13** gets the formula **=G-B*COS(RADIANS(I))**, where **I** is the right-side element angle. Note that *Excel* use radians rather than degrees in trigonometry calculations.

We define the diameter of the wire with the equation **=K** and the segmentation number cells **I11** and **I13** by the **AutoSeg** option using the variable **J**. In cell **I12**, we set it manually to **3** segments. Why 3 and not 1? If you take 1, *EZNEC* will warn you about it with the message *"Source 1: Adjacent seg different len or dia."* You may not connect a segment with the source to a wire with a different segmentation length or diameter.

Suppose your mast for hanging your inverted **V** is only 10 meters high; then the antenna ends will be too close to the ground. You can slant (rotate) the two inverted **V** arms to prevent this. You can change this low wire end height with the **Rotate Wires** option. **Figure 4c** shows the dialog box to define the rotation parameters. Thus, we rotate **All Wires** in the **CW** direction about the *X*-axis with the degrees defined in variable **D**. The rotating point is at ***Y*(m) 0** meters and ***Z*(m)** height defined in variable **G**. You must click **Apply**. It is always recommended to use **View Ant** to have control if everything is rotated as it must. Finally, click **Close**.

After the wires rotation and opening the *Wires* sheet, you shall notice a few changes and additions, see **Figure 4d**. Rows 17, 18, and 19 now become W1, W2, and W3. Most coordinates are equal to the originals in rows 11, 12, and 13. However, when you select a cell displaying the same value (as cell **B17**), you now notice the equation **=$B$11** instead of the formula **=B*SIN(RADIANS(H))**. Here **=$B$11** refers to cell **B11** and uses whatever is defined in this cell. When you select a cell with a different value than the original (as cell **D17**), you see a formula *AutoEZ* generated by the action of the

Rotate Wires. The formula is **=ROUND(($C$11 – (0)) * SIN(RADIANS(–D)) + ($D$11 - (G)) * COS(RADIANS(–D)) + (G); 9)** where **$C$11** and **$D$11** refers to the respective cells.

You also notice in column **A** a few times the **rx** characters. The **rx** stands for rotated about this *X*-axis. Marked with an arrow pointing to column A, you see *"If marked here do not write to file."* That means *EZNEC* will not use any data from these marked rows directly in the calculations. Only the **Wires** and the **Insr Objs** sheets have that option. Using that option can be a clever trick for switching in or out wires or insertion objects.

I recommend exercising the model [inverted-1.weq in **www.arrl.org/QEXfiles**] and comparing the results. You can create a horizontal or a vertical or a slanted dipole, an inverted **V** or a **V**, an **L** or inverted **L**, a one-radial ground plane, or a one-radial vertical by using the variables **D, G, H, I,** and **K**. Study additional the results by using different ground qualities and *Wire Loss*, such as aluminum instead of copper, etc.

Additional examples

Part 2 of his article contains additional models. Also see many more models in **www.arrl.org/QEXfiles**.

Conclusions

Once you get familiar with the versatile options of *AutoEZ*, you will wonder how you previously managed to model antennas using *EZNEC* alone. I wrote this article intending to pull *EZNEC* users to start an exploration of another way to model antennas by the use of variables and equations. That option was a deficiency of *EZNEC*, but Dan Maguire, AC6LA, solved this shortcoming with his *AutoEZ Excel* application. I have been using *AutoEZ* since 2014, and I must acknowledge I cannot model antennas without *AutoEZ* anymore.

I used only a handful of model examples to demonstrate several *AutoEZ* features and the strength of using variables and equations. More examples are in Part 2, and more than a hundred extra models and options are fully explained on Dan's website, **Notes [1].** This collection of models and examples is a vast goldmine for future *AutoEZ* users.

Marcel De Canck, ON5AU, built his first crystal radio set at age 12. By age 14 he was repairing defective radio sets for neighbors and relatives. Marcel became a member of the UBA (Union Belgium Amateurs), and in 1961 at age 18, I obtained the license ON5AU. He worked as a radio and TV repair technician in a local company. In 1974 he became interested in microprocessors, microcomputers, and computer programming. During that same year, he worked as a maintenance technician at the Bell Telephone Company Belgium. Later, Marcel became a field repair technician. He retired in 2000, and devoted more time to amateur radio. During 2001 to 2016 he wrote monthly columns at the "AntenneX Online Magazine" about radio wave propagation and practical antennas. His other hobbies are photography, reading, writing, traveling, gardening, and home brewing ham equipment and antennas.

Bibliography

L. B.Cebik, W4RNL, "*A Beginners Guide to Modeling with NEC.*"

Part 1: Getting settled and getting started; *QST* Nov. 2000.

Part 2: The Ins and Outs of Modeling; *QST* Dec. 2000.

Part 3: Sources, grounds, and sweeps; *QST* Jan. 2001.

Part 4: Loads, transmission lines, tests, and limitations; *QST* Feb. 2001.

L. B.Cebik, W4RNL, "*Modeling By Equation*," AntenneX, Antenna Modeling.

Issue 27: A. A Beginning.

Issue 28: B. Bigger and Better Things.

Issue 29: C. Formulas and Blocks.

Issue 30: D. Scratch Pads and Coordinates.

Any article or Ebook ever published by L. B . Cebik is available at: **www.on5au.be/Cebik documents.html**.

W. Silver, NØAX, *Antenna Modeling for Beginners. An introduction Guide to using Modeling Software*, ARRL publication 2012.

G. Ordy, W8WWW, "How to Start Modeling Antennas using *EZNEC*." Dayton, May 19, 2011, Symposium. **www.arrl.org/files/file/Antenna%20Modeling%20for%20Beginners%20Supplemental%20Files/EZNEC%20Modeling%20Tutorial%20by%20W8WWV.pdf**.

Notes

[1] The complete set of manual and model files using AutoEZ:, **ac6la.com/autoez.html**

[2] Monopole Tower: **www.on5au.be/practical-antenna-modeling.html.**

[3] Helix creation :**www.on5au.be/advanced_modeling_book.html**

[4] Moving a helix construction, **www.on5au.be/practical-antenna-modeling.html**

[5] Coil 64: Coil32 - the coil inductance calculator.

[6] M. E. Cram, W8NUE, "Small Transmitting Loop Antennas: a Different Perspective on Determining Q and Efficiency," *QEX* July/Aug., 2018, pp. 3 – 8.

[7] K. Siwiak, KE4PT, and R. Quick, W4RQ, "Small Gap-resonated HF Loop Antenna Fed by a Secondary Loop," *QEX*, July/Aug. 2018, pp. 12 – 17.

[8] K. Siwiak, KE4PT, and R. Quick, W4RQ, "Small Gap-resonated HF Loop Antenna," *QST* Sept., 2018, pp. 30 – 33.

Jacek Pawlowski, SP3L
Drzonkow - Krucza 6, 66-004 Zielona Gora, Poland | **jacek.sp3l@gmail.com**

The LPi – an End-Fed Antenna With Adjustable Bandwidth

It is amazing what you can achieve with three closely-spaced wires.

The prototype of the LPi has been built for the 21-29.7 MHz frequency range. Note how small the cross-arms are and how little space this antenna occupies.

Sometimes, it is more convenient to use an end-fed antenna rather than a center-fed dipole/doublet. That's especially true when speaking about verticals. However, end-fed antennas often need RF ground or elevated counterpoises to operate. In my QTH conditions, this is a serious disadvantage. So, I have always been very interested in end-fed antennas with built-in counterpoises. Such antennas are often referred to as "self-contained" or "ground-independent."

The antenna presented in this article is ground-independent. It requires neither a system of ground radials nor elevated counterpoise to work. Also, the shield of the coaxial cable feeding the antenna does not act as a hidden counterpoise. A common-mode choke is supposed to be installed at the antenna feed point to prevent excitation of the common-mode current in the feed line (excitation by conduction). But that's just the first interesting feature of this design. There are more to come.

Antenna geometry

The antenna is surprisingly simple, see **Figure 1**. It looks like a small upper-case letter L followed by a large upper-case Greek letter Π, hence I call it LPi. At first glance, the LPi may appear to be a derivative of an end-fed Zepp folded in half. However, the proportions of the wires lengths in the LPi are different, see **Figure 2**.

Due to such proportions and close proximity of the wires, the currents flowing in the LPi wires are not just in-phase or out-of-

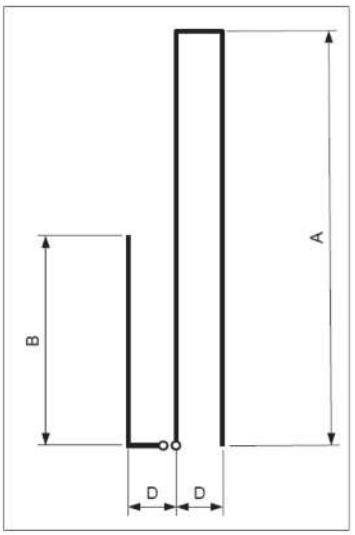

Figure 1 — The LPi antenna shape. In reality, dimension D is much smaller in comparison to A and B than shown in the picture.

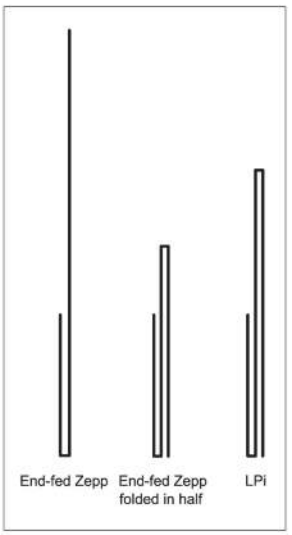

Figure 2 — The LPi antenna compared to an end-fed Zepp and an end-fed Zepp folded in half.

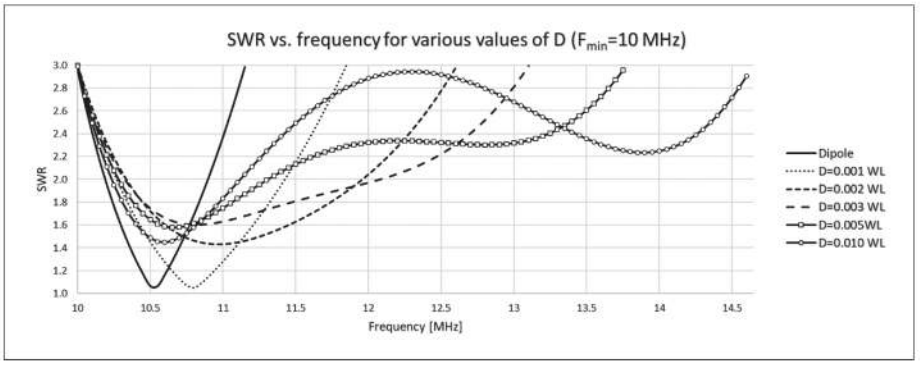

Figure 3 — The LPi antenna SWR plots for various values of D. The dipole SWR plot has been also included for reference. 200 Ω impedance source has been assumed for the LPi and 75 Ω source for the dipole. Simulations ran in free space.

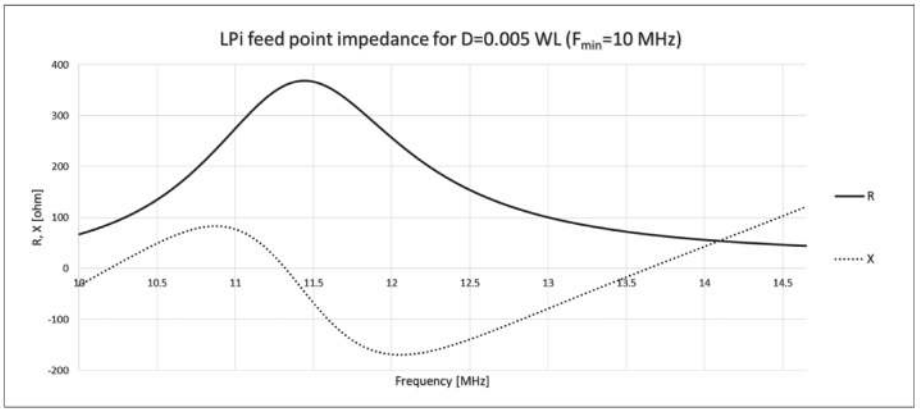

Figure 4 — The LPi antenna feed point impedance plot reveals not one but three resonances within the operating frequency range. Calculated for D=0.005 *WL*.

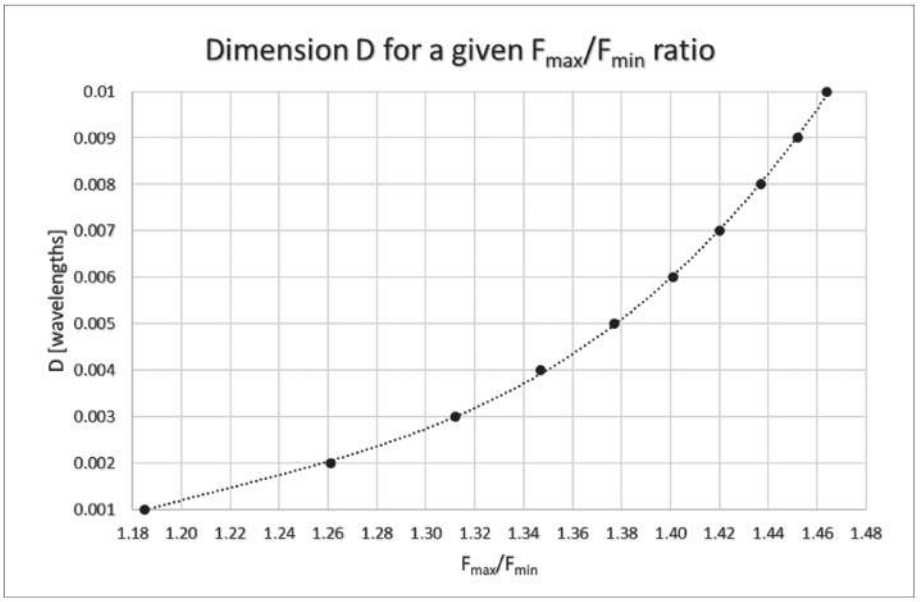

Figure 5 — Dimension D required for a given *Fmax/Fmin* ratio.

phase referred to the signal source (as in many classic antennas) but they have continuously varying phase shifts if one moves between the bottom and the top of the antenna. Interaction between the LPi wires is really complex and it is virtually impossible to guess the antenna performance without modeling it in a simulator.

Simulation results

As simulations revealed, the LPi radiation pattern is very much dipole-like. Its overall length (height) is a little smaller than a half-wave for the operating frequencies so naturally, its gain is a split decibel smaller that the gain of a half-wave dipole at the lowest operating frequency. All that is not a big surprise. What is very surprising though is the fact that depending on the A, B and D dimension ratios, the antenna has various SWR bandwidth. Also, this bandwidth can be much larger than that of a classic half-wave dipole.

For the purpose of this article, we will use SWR=3 bandwidth rather than the more often used SWR=2 bandwidth. Limiting SWR to 3:1 guarantees that every modern transceiver equipped with an internal antenna tuning unit will be able to match its transmitter output to the antenna and, at the same time, additional signal loss in a feed line (due to SWR greater than 1:1) will not be too high.

A regular center-fed half-wave dipole has the *Fmax/Fmin* ratio equal to 111.5% where *Fmax* and *Fmin* are the maximum and minimum frequencies of the range in which SWR ≤ 3. The LPi antenna outperforms the dipole significantly. It can achieve the *Fmax/Fmin* ratio as high as 146.4%. These calculations are valid for wire diameter 2 mm and minimum frequency 10 MHz, see **Figure 3**.

The SWR plots shown in **Figure 3** were obtained in the following way. The minimum frequency *Fmin* was assumed to be equal to 10 MHz. The wavelength (*WL*) for this frequency is equal to 30 m in accordance with the formula:

WL [m] = 300 / *Fmin* [MHz]

The antenna dimension D was varied from 0.001 *WL* through 0.010 *WL* (from 3 cm through 30 cm). For every given value of D, dimensions A and B were adjusted to achieve SWR ≤ 3:1 in the frequency range starting from *Fmin* upwards. It was observed that each time D was increased, the maximum frequency *Fmax* increased too. For the minimal value of D=0.001 *WL* (3 cm), *Fmax* was equal to 11.85 MHz. And for the maximum value of D=0.01 *WL* (30 cm), *Fmax* was equal to 14.64 MHz.

To understand what causes such a large bandwidth, let's examine the feed point impedance plot (**Figure 4**). The antenna has three resonances: near the beginning, near the center and near the end of the operating range. At the same time, the resistive component of the impedance changes very moderately from about 70 Ω to about 370 Ω. Moreover, the reactance values are quite moderate too. Thanks to that, if you connect a source having 200 Ω internal resistance to this antenna, you will get SWR < 3:1 over a wide frequency range.

LPi design procedure

To find the LPi dimensions for a desired frequency range, you must first select the *Fmin* and *Fmax* frequencies in such a way that their ratio *Fmax/Fmin* is within the range 118.5% to 146.4%. You then read the corresponding value D from the plot in **Figure 5**. Knowing D, you read the A and B values in **Figure 6**. Finally, you convert A, B and D values from wavelengths to meters. You do that by multiplying them by the wavelength calculated for *Fmin*. See the aforementioned formula for *WL*.

The dimensions found in this way are correct only for the frequencies close to the 10 to 15 MHz range and for the conductor diameter close to 2 mm. If you use this method for quite different frequencies (like 1.8 MHz or 28 MHz) without scaling up or down the antenna wire diameter accordingly to the new frequency, the obtained dimensions will not be perfectly accurate. In a situation like that, I recommend using antenna simulation software to fine tune dimensions A and B. The most convenient software is the combination of *EZNEC Pro+ v. 7.0* and *AutoEZ* applications. The "Optimize" function included in the *AutoEZ* does a great job in fine tuning the dimensions.

I created a number of reference designs for various frequency ranges for the hams less advanced in computer aided antenna simulation. **Table 1** lists the dimensions achieved in the optimization process. All reference designs assume bare copper wires of the same diameter. If you prefer to use insulated wires, leave D as it is, but reduce A and B by 3%.

Table 1 — LPi reference designs for the frequency ranges useful for HF bands.

Band, m	Fmin, MHz	Fmax, MHz	A, m	B, m	D, m	Wire type
160	1.7	2.1	77.46	39.85	0.125	A
75/80	3.33	4.27	38.75	19.58	0.111	B
60	4.7	5.9	27.65	14.06	0.063	B
60+40	5	7.5	23.50	10.97	0.666	B
40	6.43	8.03	20.25	10.26	0.060	B
40+30	6.96	10.2	17.28	7.50	0.430	B
30	9.15	11.2	14.32	7.23	0.041	B
30+20	9.9	14.5	12.13	5.32	0.302	B
20	13	15.4	10.21	5.19	0.023	B
20+17	13.7	18.5	9.04	4.43	0.091	B
17	16.9	19.7	7.89	4.01	0.019	B
17+15	17.7	22	7.33	3.85	0.038	B
17+15+12	17.9	25.2	6.77	3.08	0.154	B
15	19.5	23.5	6.76	3.55	0.024	B
15+12	20.3	26.4	6.25	3.12	0.055	B
15+12+10	20.8	30	5.77	2.61	0.144	B
12	23.5	27	5.68	2.79	0.015	B
12+10	24.3	30.6	5.28	2.70	0.037	B
10	27	31.3	4.94	2.52	0.015	B

Wire type A: Cu 6 mm² (d=2.8 mm) or #10 AWB, no insulation
Wire type B: Cu 2.5 mm² (d=1.8 mm) or #13 AWB, no insulation

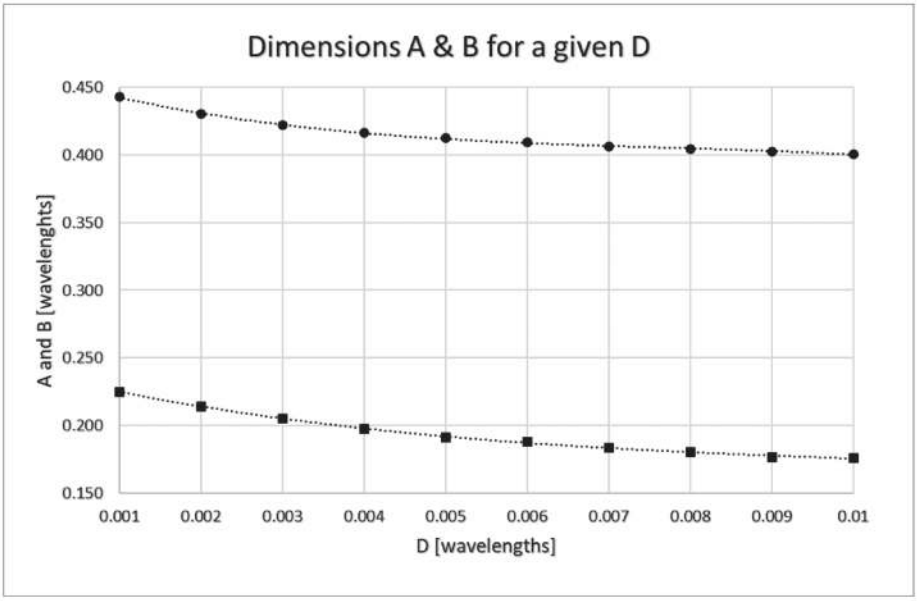

Figure 6 — Dimension A (top curve) and B (bottom curve) as a function of D.

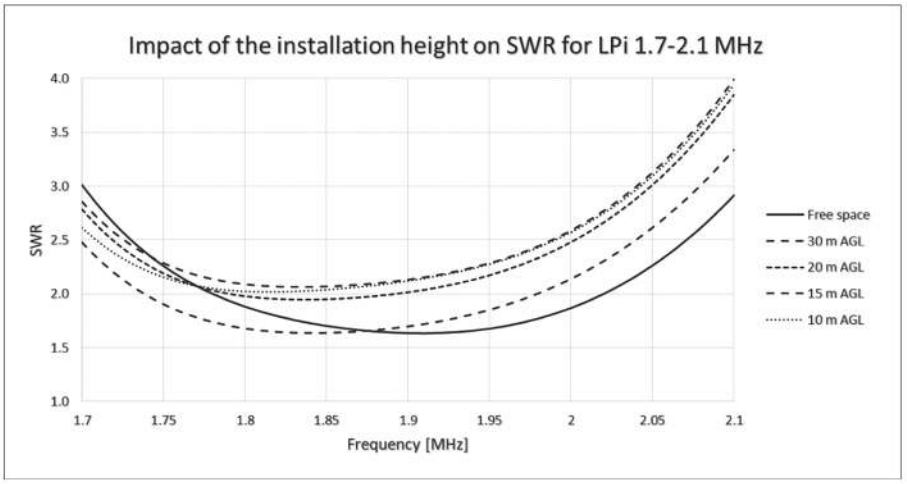

Figure 7 — Changes in SWR for a horizontally mounted LPi calculated for 160 m band for different heights above ground level (AGL).

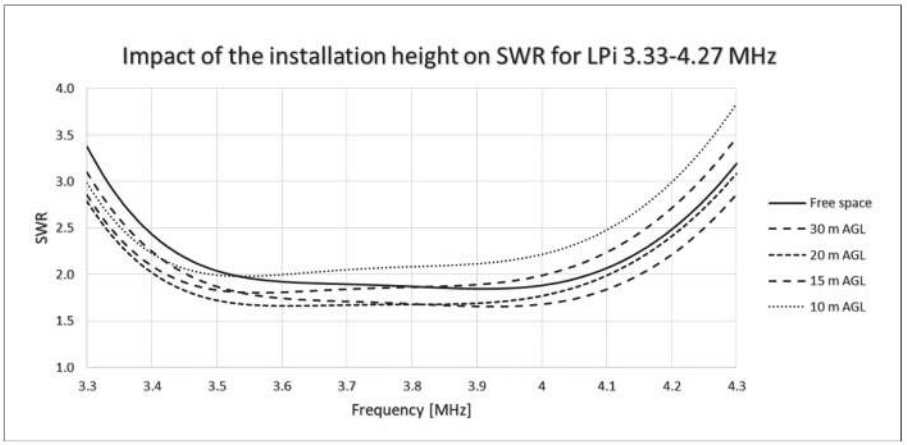

Figure 8 — Changes in SWR for a horizontally mounted LPi calculated for 75/80 m band for different heights above ground level (AGL).

Impact of ground

So far, we were analyzing the LPi performance in free space because this is a common practice when comparing a newly designed antenna with a reference antenna like a dipole. But in the real world, antennas do not always operate in free space. So, it is worth checking out how much the proximity of ground changes performance of the LPi. I first examined horizontally mounted antennas having the dimensions taken from **Table 1**.

The simulations have shown that you do not have to worry about SWR increase even for the 160 m or 75/80 m band antennas installed horizontally at low heights (see **Figures 7** and **8**). Impact of ground was even less noticeable at higher bands. This antenna tolerates ground proximity quite well.

For vertical installations, you do not have to worry about SWR. The impact of ground is negligible.

Taming common-mode current

The imbalance of the currents flowing in the inner and outer conductors of the coax is called common-mode current. Common-mode current in a feed line is not desired and there are ways to minimize it.

What I recommend to use in the LPi matching network is a 4:1 voltage unun followed by a common-mode choke, both

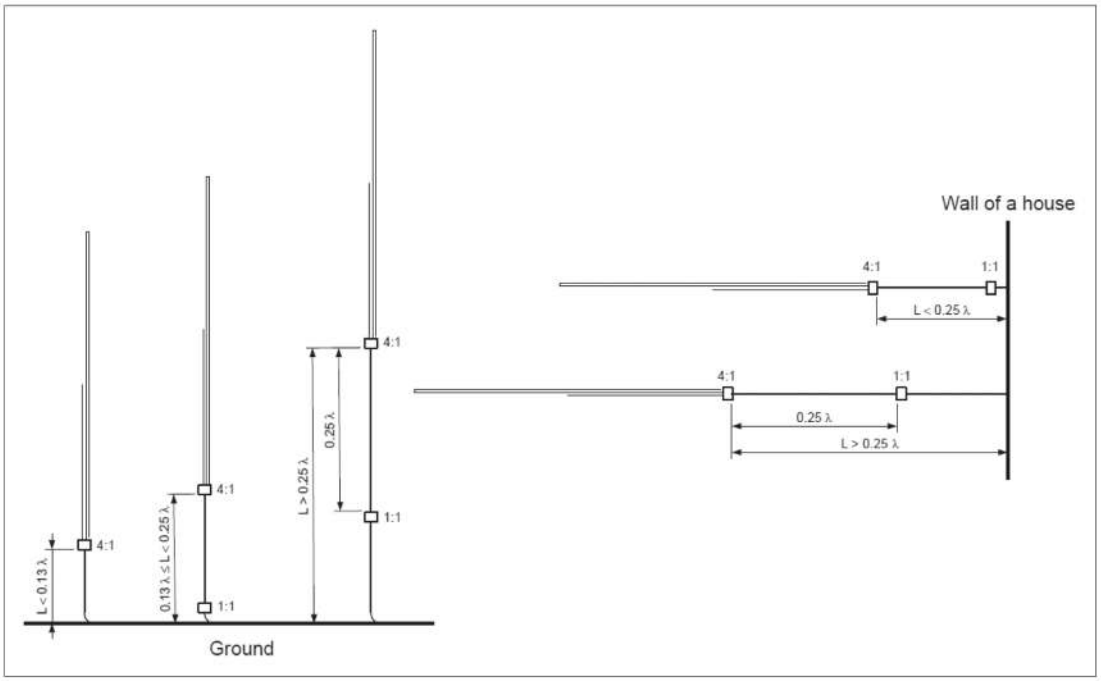

Figure 9 — Recommended placement of an additional choke (1:1 current balun) depending on the distance between the matching network (denoted here as 4:1) and the spot where the coax touches ground for the first time or where it runs through a wall.

wound with a thin coax. A common-mode choke is sometimes called 1:1 current balun or line isolator. You need two toroidal cores to construct the matching network. For low input power (up to 200 W) 1.4" O.D., ferrite cores of the 43 material from Fair-Rite will be okay.

Common-mode current can also be excited by radiation. In other words, it can be induced on the coax shield due to electromagnetic radiation from the antenna. Such induction is much more likely to happen in asymmetrically fed antennas than in symmetrical systems. You can counteract it by inserting an additional common-mode choke in the coax at some distance from the feed point. The additional choke is not always needed. **Figure 9** shows where I would recommend to connect it depending on antenna installation conditions.

Please note that this time I used not *WL* but λ symbol to denote wavelength. That's because λ is referred not to F_{min} (as the *WL* was) but to the maximum operating frequency *Fopmax* you expect to use:

λ [m] = 300 / *Fopmax* [MHz]

For example, if the highest band is 10 m, then *Fopmax* = 29.7 MHz and λ= 10.1 m.

If the coax measures less than 0.13 λ between the feed point and the spot where you can consider the coax shield grounded via capacitive coupling to ground, you do not need to use an extra choke at all. Such situation is typical for a vertical LPi mounted low above the ground. But if the LPi is mounted higher, and the coax between the matching network and ground measures 0.13 to 0.25 λ, I recommend connecting an extra choke just above the ground touching spot. If the distance is even larger, insert such a choke 0.25 λ away from the feed point.

The LPi can also be installed in such a way that the coax does not touch ground anywhere between the feed point and the wall of a building. If so, measure the coax length from the feed point to the wall. If it is shorter than 0.25 λ, add a choke just before the wall. If it is longer, add a choke after 0.25 λ measured from the feed point, no matter how long the coax is.

Prototype antenna

When a new antenna type is proposed, it is always very desirable to build and test a real antenna to make sure the simulations were accurate. The **lead photo** shows a prototype LPi antenna mounted on my balcony railing. The antenna was made of copper wires of 1.8 mm diameter. I used a fiberglass pole as a main support and three plastic crossarms to fix the wires in place.

The prototype antenna covers 15, 12 and 10 m bands. Initially, its dimensions were as those in the **Table 1**. During trimming, I reduced A from 5.77 to 5.59 m and B from 2.61 to 2.49 m. D remained unchanged: 0.144 m.

Figure 10 shows the SWR measurement results of the real antenna. At the beginning, I measured the antenna impedance at its feed point with an antenna analyzer connected directly to it with very short wires (no coaxial cable at all). I exported the resistance (*R*) and reactance (*X*) measurement results stored by the analyzer to the *Zplots* application and calculated what the SWR would be if the signal source impedance was 200 Ω. This SWR is shown with a dotted line in **Figure 10**. The SWR stayed below 3:1 in the range 20.5 to 30 MHz.

Exactly such bandwidth would be achieved with a 50 Ω source if an ideal 4:1 matching network was connected to the antenna. However, when I added a real matching network and measured SWR at its output, the plot I got was not identical with the previous one. See the solid line plot in **Figure 10**. Evidently, my network was not ideal. I used a 4:1 unun wound with RG174 coax on a 43 material core, followed by a common-

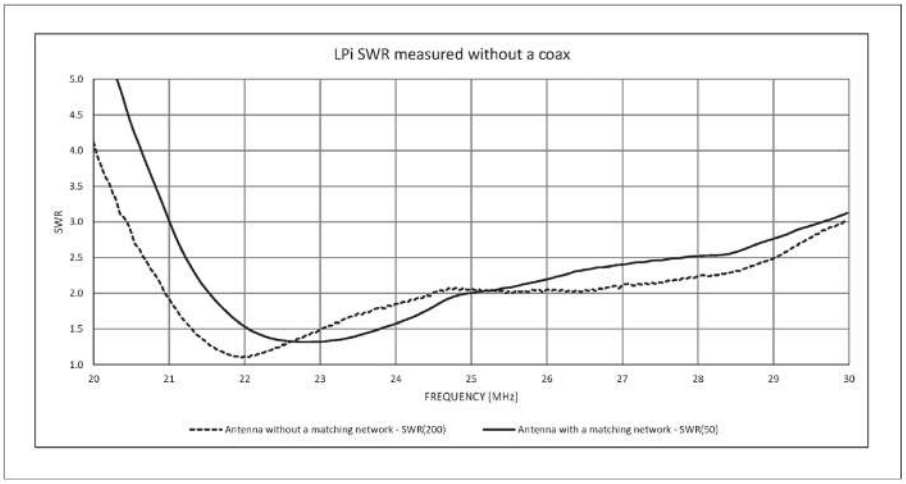

Figure 10 — The LPi SWR measured without any coax.

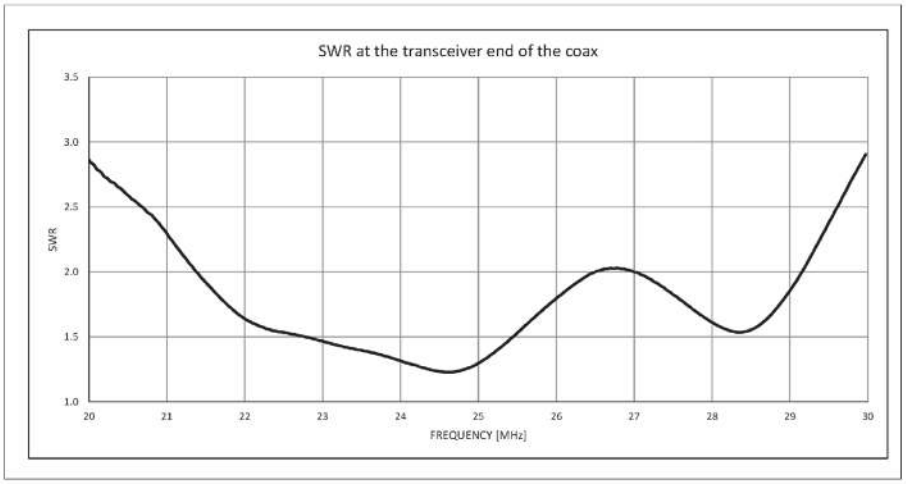

Figure 11 — SWR measured with 22 meters of low loss coax connected to the antenna.

mode choke wound on the same core type with the same coax type. I tested a number of other versions of the matching networks, but the above one was the best.

When the LPi is fed via a coax its SWR decreases because a coax is a lossy feed line. This is visible in **Figure 11**. With 22 m of low loss 5.4 mm diameter coax connected to the matching network, the SWR measured at the TRX port was below 2.5:1 for any frequency between 21 through 29.7 MHz. I considered such SWR values as satisfactory.

I must add here that I did not neglect my own recommendation. I inserted an additional common-mode choke 2.5 meters away from the antenna.

The on the air tests I conducted on 15 m band listening to **websdr** receivers located in the other countries proved that the prototype antenna gain was at least as good as the gain of my old 3/8 λ GP which I used as a reference. The LPi worked as expected.

In addition to the antenna shown in the **lead photo**, I built another prototype. This one had the central conductor made of aluminum tubing and the side conductors with copper wires. So, the central conductor had much larger diameter than the side conductors. The simulations showed that such an antenna required different A, B and D dimensions than those in **Table 1**. Its feed point impedance was closer to 100 Ω rather than 200 Ω. To my disappointment, the real antenna performance differed significantly from the computer modeling. I am not going to analyze this case in detail here. It seems that you cannot trust simulation results if you use conductors of different diameters in the LPi antenna model. After a tedious process of trial and error, one could make such an antenna work in the end. But I was not patient enough and disassembled it.

Final thoughts

The LPi is an end-fed antenna with many interesting features. It is ground-independent and is very slim. If used as a vertically polarized antenna, it can be installed in places where a GP antenna does not fit due to space required for its counterpoise. The LPi radiation pattern and gain are very close to that of a regular half-wave dipole. Ground proximity affects the antenna SWR performance in a very moderate way. It is possible to adjust the LPi bandwidth by changing its proportions. This bandwidth can be really awesome; large enough to cover two or, in some cases, even three neighboring ham bands.

You can successfully simulate this antenna with a *NEC*-5 based simulator provided that all antenna wires are of the same diameter. Simulation with a *NEC*-2 based simulator is also accurate if you create the antenna model in accordance with modeling guidelines. I also tried *MMANA-GAL* with *MiniNEC* engine and got very similar simulation results.

Building and trimming the real LPi was not difficult. You can do the trimming by shortening dimensions A and B by the same amount, for example in 0.003 *WL* steps or so.

You should follow the normal recommendations when finding the operating position for a vertically polarized antenna. If you have buildings, metallic fences and similar object obstructing low angle radiation, consider mounting the LPi not just above the ground but higher. After all, this is a ground-independent antenna, so why not to take advantage of that?

Place it away from objects like lamp-posts, metallic gutters, and walls of buildings. If you do not, not only its gain and radiation pattern will suffer but also its SWR bandwidth may not be as wide as predicted. As you can see in the **lead photo**, I installed my prototype antenna on a balcony with a metal railing. This is not the most desirable position. Despite that, my antenna works very well. I can honestly recommend this design for everybody.

Jacek Pawlowski, SP3L, is an electronics engineer with a MSc degree. He started his professional career as an electronic designer in testing and measurements. After about 15 years as a circuit and PCB designer, he switched to a management career path. He has been a research and development project department manager in several companies since then. Jacek caught his radio bug when he was still in primary school in the early 1970s. In 1978 to 1999 he was active as SP3LFV. After that he stepped away from the hobby for 15 years. In 2014, he became active again as SP3L. Jacek maintains a web page, ***https://sites.google.com/view/sp3l-hf-antennas/home-page****.*

Upcoming Conferences

Utah Digital Communications Conference

February 3, 2024
Sandy Utah

www.utah-dcc.org

The Utah Digital Communications Conference will be held at the Salt Lake Community College, Larry H. Miller Campus, in Sandy, Utah, February 3, 2024. Check website for details.

SCaLE 21x

March 14 – 17, 2023
Pasadena, CA

www.socallinuxexpo.org/scale/21x

The 21st Annual Southern California Linux Expo (SCaLE 21x) will be held at the Pasadena Convention Center in Pasadena, CA, March 14 – 17, 2024. Check website for details.

Michael Reinhold, HB9BEP
Rehweg 1, 9472 Grabs, Switzerland | **hb9bep@uska.ch**

Martin Klaper, HB9ARK
Scheimatte 22, CH-4616 Kappel, Switzerland
hb9ark@uska.ch

FT8 Contacts and Ionospheric Radio Propagation Analysis

Systematic collection of S/N reports in modern digital modulation schemes like FT8 provides deeper insight into shortwave propagation across the ionosphere.

This study shows how recent progress in ham-radio hardware and software can be used to quantitatively investigate shortwave DX propagation via the ionosphere. Modern digital modulation schemes like FT8 allow not only the parallel acquisition of up to 40 communications channels in a 2.5 kHz bandwidth but also give the amateur quantitative and reproducible data about actual S/N ratio experienced in an individual channel. Even though S/N is measured on a relative and not on an absolute scale, we are able to investigate interesting aspects about ionospheric radio wave propagation over long distances. When collecting thousands FT8 contacts during the recent solar spot minimum, we noticed that east-west as well as west-east DX propagation, with both stations at about the same middle northern latitude, seemed not to be symmetrical regarding S/N reported in FT8. Theory suggests that about the same S/N ratio should be experienced under equivalent technical and ionospheric conditions at both ends. A review of both professional and amateur radio literature seldom mentions this phenomenon. To close this gap, we recorded and statistically analyzed 984 unique FT8 contacts between Switzerland and Japan starting June 2019 and ending in December 2021. This study makes three contributions: (1) for the 9,500 km path between Switzerland and Japan shortwave ionospheric propagation is symmetrical in the average, (2) it is positively correlated with daily sunspot numbers, and (3) is not correlated with planetary Ap index. Finally, FT8 gives the radio amateur a novel tool to contribute to quantitative propagation research.

1 – Introduction

With the first successful radio transmission between Poldhu in Cornwall and St. John's in Canada in 1912, Guglielmo Marconi provided the proof of concept for the feasibility of long-distance communication with electromagnetic waves. The big advantages of this novel technology over the use of signals sent via copper cables were: (1) the attenuation of the signal power over the distance r is proportional to $(1/r)^2$ and not to $\exp(-r)$, and (2) the bandwidth for signal transmission is much higher than with traditional wire technology. (3) Since radio is not bound to a fixed network of wires, connecting the transmitting and receiving sites any location, even on high seas, can be chosen. The adoption of this new technology and its worldwide diffusion took about a decade and was accelerated using ship to shore communications especially in emergency cases. Early ham radio operators thereafter proved the feasibility of shortwave communication over long distances and this hitherto unexpected phenomenon had to be understood. Obviously, radio waves did not only follow the curvature of the earth but also were confined within the earth and a reflecting medium called "the ionosphere" several hundred km above ground. This enabled worldwide communications between any two points on earth. Radio propagation science was born. Ever since, the ham radio community has contributed to progress of this field.

This article contributes to existing ionospheric propagation studies of ham radio operators in several ways: (1) we show that S/N contact data of DX contacts with FT8 stations provide useful information about band openings to certain limited areas of the world, and (2) that no matter how strong or weak any DX station in such area can be heard, any prior guess about the S/N of our signal upon answering that call is futile, because of the overwhelming variability of ionospheric pathways. (3) Assuming similar technical working conditions on both ends of the ionospheric path the statistical average of both S/N reports will be about equal. This hypothesis is tested with the sample of 984 FT8 unique DX contacts on 14, 21 and 28 MHz between the station HB9BEP in Switzerland and the partner stations all located in Japan. A quantitative statistical analysis of our sample is presented. Finally, we present our results and discuss our main findings and practical and theoretical implications along with study limitations and suggestions for future research.

2 – Methodology: Data Collection and Sample

A total of 9,000 FT8 worldwide contacts with more than 120 countries/entities were logged and collected in a database between June 6, 2019, and December 25, 2021, by the station HB9BEP to qualify for the digital mode DXCC of the *ARRL*. Each contact was made in person, without the use of automation software. The collection of all 9,000 FT8 log entries from all over the world is too varied to derive any novel information about ionospheric radio propagation from it. As outlined above we wanted to test the hypotheses formulated above and therefore a proper subsample of all contacts had to be extracted. Anything else would mean to compare apples and oranges.

Japan, see **Figure 1**, was chosen as a target area for the following reasons.

- The location of station HB9BEP is in the Swiss alps and Japan is luckily in a favorable beam direction for DX contacts due to low contours at the horizon. In terms of noise levels this QTH can be qualified as "rural" **[1]**. This is not true for the Japanese stations contacted, especially in the Tokyo and Osaka regions.
- A total of 984 FT8 connections were extracted from the database, the biggest number of any of all distinct DX-entities contacted. For statistical analyses sample size does matter. The more, the better since it allows the further formation of groups of similar objects for the analysis like groups of stations in the same call sign district. Geophysics data, like sunspot numbers and Ap indices, were imported from a database maintained since 1932 by the GFZ German Research Center for Geosciences in Potsdam, Germany **[2]**.
- All of Japan can be reached from Switzerland by radio in a narrow horizontal angular spread around 30° N and the average distance to all partners lies around 9,500 km. This restricts the target area and results become more comparable. The beam width of our 3-element Yagi covered this area easily.
- The great circle path does not touch the aurora borealis region which may influence ionospheric propagation. This contrasts with the path from Switzerland to the US and Canadian westcoast which is sometimes strongly affected by the aurora phenomenon.
- Japan is the country with the largest number of active ham radio operators in the world with more than 1.2 million. licensees. In our context we are concerned with only about 120,000 Japanese hams that are allowed the privilege of operation in the traditional 20/15 and 10 m bands. We have so far not yet exhausted the potential for unique contacts in the 10, 15 and 20 m bands. In **[3]** the enigma of the Japanese call sign system is unraveled (in English) together with all details like the allocation of numbers in the call sign to geographical districts.
- Japan has divided the country in ten geographically different call sign districts. The number in the call sign ranges therefore from 0 to 9. Number "1" is used in the Tokyo area and "3" for the Osaka area. Unlike the US, the encoding of the number in the call is strictly enforced. We used this property in our statistics for further grouping of our contacts. We used this as a proxy for the actual great circle distance. The four digits code out of six for the QTH in FT8 telegrams is simply too coarse for our purpose.
- All DX contacts with Japan were essentially three-hop ionospheric propagation paths of the radio waves. This was confirmed by sample tests with the propagation program *ProLab Pro v.3.1* **[4]**.
- In our case the Japanese regulations regarding ham radio operation and license classes are very similar to the ones in Switzerland. Maximum RF power allowed is 1 kW in both countries.
- Ham radio equipment in both places originates essentially from the same manufacturer's oligopoly. HB9BEP used a Japanese Kenwood TS-590 SG together with a commercial 3-element 3-band Yagi for 20, 15 and 10 m. This is quite on equal terms with Japanese stations. Since actual working conditions, like RF power and antenna, are not relayed in FT8 contacts, we must leave out this aspect. Whether this is really an issue will be discussed later in this text.
- As Hunsucker and Hargreaves pointed out, there are three latitude regions in the Northern and Southern Hemisphere where ionospheric propagation is quite different and distinct: (1) polar, (2) middle and (3) tropical latitudes **[5]**. In this respect our choice of Switzerland and Japan for these studies is quite reasonable.

Next, we show our results, and discuss our main findings.

3 – Results

To calculate the statistics of our data we used the open-source software package "*R*" **[6]**. **Figure 2** shows the histogram of the signal reports received by all 984 contacts made on 14, 21 and 28 MHz with Japanese stations. The bin width is 1 dB and the

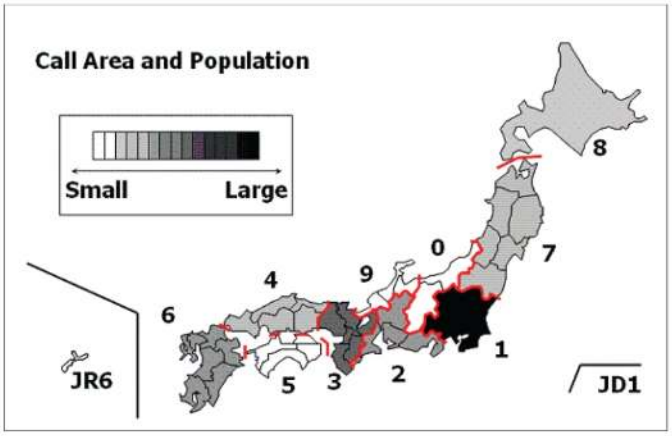

Figure 1 — Call Area Districts (CSD) in Japan.

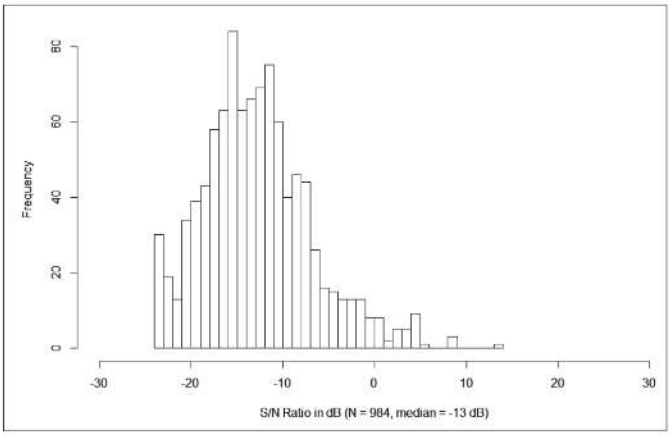

Figure 2 — Histogram FT8 Signal Reports received from Japan (20, 15, 10 m).

range goes from –24 dB, which is the lowest S/N ratio reported up to +14 dB as the highest. The median is –13 dB on the FT8 scale.

Figure 3 shows the histogram of the signal reports sent to all 984 contacts made on 14, 21 and 28 MHz with Japanese stations. The statistics are similar to those in **Figure 2**.

The next histogram, **Figure 4**, is the ratio of S/N reports sent in dB minus the S/N report received in dB by the same station. Since the dB scale is logarithmic, forming differences is the same as calculating numerical ratios. Thus for the bin at –20 dB this means that our report sent was –20 dB below the report obtained from the identical station. At 0 dB, which is equal to 1, both reports would have been the same, no matter how big or small. The statistical relevance of this result is high since all the 984 contacts are unique on the same band. Comparing this with public polls means that no interviewed person was questioned twice or even more "on the same band." Looking at the histogram from the perspective of standard statistics the median of all individual samples is at –2 dB. This means that in the average the reports sent and received are equal. This is exactly what we wanted to know. **Figure 4** also reveals something else. The absolute span of ratio is close to 40 dB, counting the extreme results it is even as high as 50 dB. For 50 % of the stations contacted the ratio of S/N is in a close range of about ±6 dB around the –2 dB median.

To push this exploratory analysis even further, we wanted to know whether the above analysis would be different when comparing the various call sign districts in Japan.

Figures 5, 6 and **7** summarize our results in the form of scatter plots for S/N received, S/N sent, and S/N received minus sent. The black dots represent the S/N of each contact, the values can be read from the vertical axis. On the horizontal axis, the call sign district (CSD) is marked from 0 to 9. What strikes you is the high number of contacts into CSD=1, the region of Tokyo with the largest number of stations in Japan. In the diagrams we combined the results from 20, 15 and 10 m bands for a grand total of 984 contacts. This step was necessary since for a reasonable statistics more than 20 sample points is the minimum required. As one counts for CSD=0 (Hokuriku district west of Tokyo) this condition is just fulfilled.

To augment this exploratory analysis, we demonstrate the influence of the ionosphere upon the S/N ratios reported by FT8 software.

We guessed that sunspot numbers, or as a better proxy F10.7 cm solar flux data, as well as planetary Ap indices are correlated with the S/N reports sent to Japan. We analyzed this for all 20, 15 and 10 m contacts separately since from theory ionospheric effects increase with frequency. The method used was a linear regression of R_SENT (the S/N report sent to Japan) versus F10.7adj and Ap taken from the Potsdam archive.

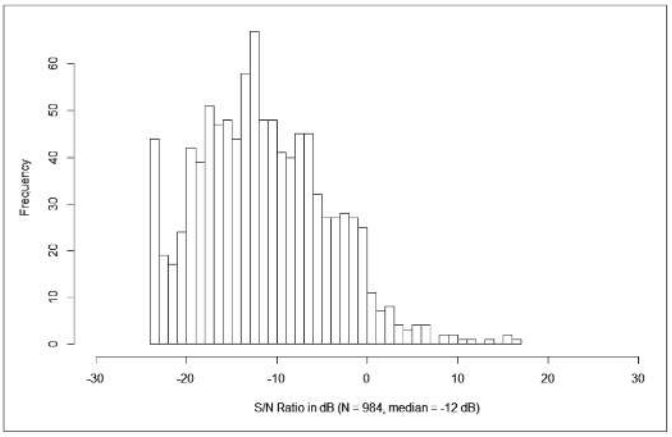

Figure 3 — Histogram FT8 Signal Reports sent to Japan (20, 15, 10 m).

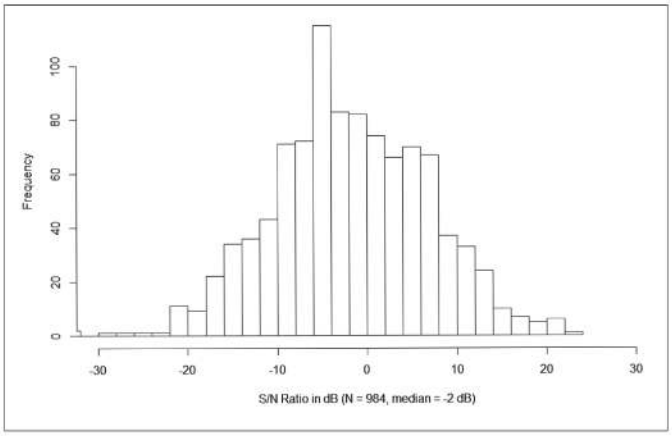

Figure 4 — Histogram FT8 Signal Reports Received minus Sent (20, 15, 10 m).

Table 1 – Output of the R-routines used on 14 MHz data set.

lm(formula = R_SENT ~ F10.7adj + Ap, data = 14 MHz, N = 473)

Coefficients:	*Estimate*	*p-value*
F10.7adj	0.15808	highly significant
Ap	–0.898	non-significant

Table 2 – Output of the R-routines used on 21 MHz data set.

lm(formula = R_SENT ~ F10.7adj + Ap, data = 21 MHz, N = 450)

Coefficients:	*Estimate*	*p-value*
F10.7adj	0.10572	highly significant
Ap	–0.19629	barely significant

Table 3 – Output of the R-routines used on 28 MHz data set.

lm(formula = R_SENT ~ F10.7adj + Ap, data = 28 MHz, N = 55)

Coefficients:	*Estimate*	*p-value*
F10.7adj	0.4196	strongly significant
Ap	–0.1892	non-significant

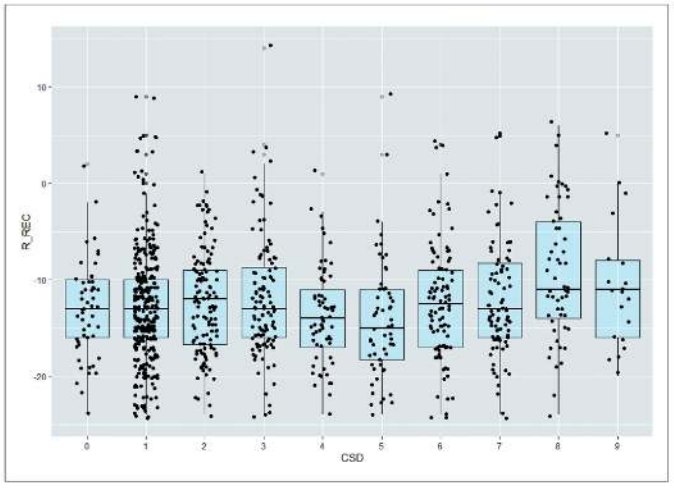

Figure 5 — Boxplot Received Signals R_REC vs. Call Sign Districts (CSD).

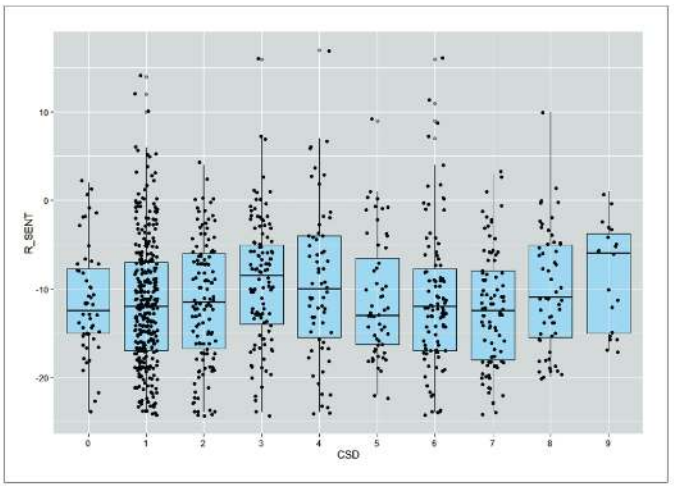

Figure 6 — Boxplot Sent Signals R_SENT vs. Call Sign Districts (CSD).

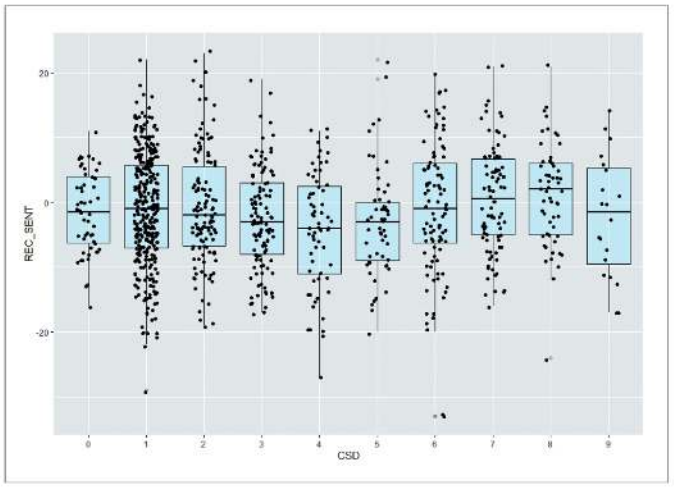

Figure 7 — Boxplot Received minus Sent Signals REC_SENT vs. Call Sign Districts (CSD).

Tables 1, 2 and **3** summarize the multivariate linear fit statistics for 14, 21 and 28 MHz.

Multivariate regressions are much more demanding to perform and interpret than univariate statistics because there is more than one variable involved. **Tables 1 – 3** show a condensed output of the R-routines used on each dataset. The first line gives the formula used for linear regression along with label of the dataset. N is the number of contact degrees of freedom to be precise. The F10.7adj estimate is the normalized regression coefficient. P-value is an indication of the degree of significance of the estimate. The same applies to the Ap coefficient estimate.

Comparing the results of 14, 21 and 28 MHz we see that there exists a clear correlation of the reports sent from Switzerland to Japan with the adjusted 10.7 cm solar flux. It is highest for 28 MHz since this band is open only when solar flux is high, which is equivalent to higher sunspot numbers. The median sunspot number SN was 21 and the F10.7adj flux, which is a good proxy to SN, was a low 77 during the observation period. There were no sunbursts leading to geomagnetic storms. The median of Ap was only 5.0 which means the geomagnetic conditions were quiet **[7]**. There was no strong magnetic storm that might have negatively influenced ionospheric propagation. Therefore, the above correlation with the Ap index is non-significant for 14, 21 and 28 MHz, too. Beware: in general correlation does not mean causation. In our case however, we know from the well understood theory of ionospheric radio wave propagation that higher sunspot numbers, or F10.7adj values are the cause of better propagation in the higher amateur bands, but not the only one. Higher Ap indices are usually observed when the sun's particle flux disturbs the earth's magnetic field and deteriorates ionospheric propagation. Of course, this study can be extended to include other numerical propagation factors provided by numerous space weather sites. But before, one must develop some theory or observation-driven hypothesis to be tested with a properly selected data set.

4 – Conclusion, Limitations, and Outlook

All three claims that are made in the beginning of this article are supported by our statistical analysis of 984 FT8 contacts from Switzerland to Japan. Data collection was very laborious since it was all made in person and not automated by software. Data preparation and analysis required a lot of statistics and software know-how. It is shown that with the limited means of a ham-radio amateur it is possible to make a useful contribution to shortwave radio propagation studies via the ionosphere. This study would not have been possible without the excellent digital communications software FT8 provided for free by Joe Taylor, K1JT, and his crew **[8]**. Measuring accurate S/N ratios still is a difficult task, even with the help of advanced signal analysis **[9]**.

Of course, this study also shows limitations. The greatest is the lack of information about the working conditions of all the Japanese stations contacted. This includes the RF power used for the contact, the antenna utilized and the local situation with the terrain. Japan has many mountains like Switzerland and the low angle DX-path to Switzerland from the antenna to the horizon can be obstructed by the surrounding terrain. This is likely one of the reasons why big asymmetries are found in the reciprocity of signal reports.

The big span of received minus sent signal reports in **Figure 7** suggests that RF power and antenna conditions are not the only

reason for this span. Going from 10 W as a QRP station to 1 kW, the maximum allowed, explains only a span of roughly 20 dB.

For the ham radio operator one fact taken from **Figure 7** is essential: even if a DX-station calling is read in FT8 with only –20 to –24 dB S/N, it is always worthwhile to give an answer. Your reply may end up easily in a S/N report that is more than 20 dB better than expected.

Whether this type of study can be extended to other shortwave DX regions is debatable. It clearly depends on the ham-radio population in the DX location. About one thousand different contacts are required for a good statistical analysis. Great circle propagation across boundaries like the auroral and magnetic equatorial zones is challenged by ionospheric effects, which are difficult to control during a statistical analysis. We experienced this when running preliminary analyses of the ionospheric DX paths from Switzerland to Indonesia near the equator, and to the west coast of the USA and Canada when touching the auroral oval.

Martin T. Klaper, Dipl. El.-Ing. ETH, HB9ARK, has been licensed since 1971. He is a member of ARRL, USKA, AMSAT-HB, AMSAT-UK, BATC, Group UHF HB9UF, Swiss-ARTG, Amateurfunkverein der Hochschule Luzern HB9HSLU, and is a professional engineer. Martin is retired professor of Computer Science at the University of Applied Sciences Lucerne. Martin has worked for 20 years in the telecom industry, and still lectures on data structures and algorithms, mobile communications and teaches ham radio classes. He enjoys the contact with his students and the many facets of amateur radio. Martin is currently involved in ground station development for satellites.

Michael Reinhold is retired with a diploma and a Ph. D. in Physics from the University of Basel, Switzerland. He has been licensed as HB9BEP since 1972, and is a member of the ARRL (ex-KG1Y), USKA, Swiss-ARTG, Group HB9GR and HB9SG, and is Life Member of the IEEE. He earned the DXCC Digital # 7,499. Prior to his retirement he worked for 20 years in high-tech industries and for another 15 years as a scientist and teacher at various universities in Switzerland (University of Berne, University of St.Gallen, ETH in Zürich). He enjoys ham radio, antenna and propagation science, deep learning, picture analysis, face-analysis, and age and sentiment recognition.

References

[1] Recommendation ITU-R P.372 provides information on the background levels of vertically polarized radio- frequency noise in the frequency range from 0.1 Hz to 100 GHz: **www.itu.int/dms/pubrec/itu-r/rec**

[2] **https://www.gfz-potsdam.de/**

[3] **www.motobayashi.net/callsign/enigma/index.html**

[4] **http://spacew.com/index.php/software/**

[5] R. D. Hunsucker, J. K. Hargreaves; "The high-latitude ionosphere and its effects on radio propagation," Cambridge Atmospheric and Space Science Series, Cambridge, 2003.

[6] See **https://cran.r-project.org**. This is a widely used software package in the scientific community.

[7] **www.spaceweatherlive.com/en/help/the-ap-index.html** gives a good explanation about Ap values and its meaning.

[8] **www.physics.princeton.edu/pulsar/k1jt/**

[9] J. Griffiths, G3ZIL; R. Robinett, AI6VN; and G. Elmore, N6GN; "Estimating LF-HF Band Noise While Acquiring WSPR Spots," *QEX*, Sep./Oct., 2020, *ARRL*, Newington, CT.

Dennis G. Sweeney, WA4LPR
1206 Westover Dr., Blacksburg, VA 24060 | **dsweeney@vt.edu**

Phase Noise Measurement Revisited

A direct method and a phase locked loop (PLL) method of measuring phase noise are described.

This paper describes two methods for measuring phase noise. The first is a direct method employing a spectrum analyzer controlled by a General Purpose Interface Bus (GPIB) and software available from KE5FX. The second uses a phase locked loop (PLL) and a phase detector. If carefully implemented, this second method is capable of performance approaching that of commercial phase noise measurement systems. In fact, it is similar to a number of commercial systems. This paper covers the analysis needed to set up this PLL based measurement and some of the practical issues that must be addressed in order to obtain consistent accurate results.

Introduction

With the advent of high dynamic range receivers, digital modulation formats that rely on small phase shifts and microwave systems that operate into the 100 GHz region and beyond, the phase noise of oscillators is becoming of more interest to amateurs.

Ideal signals are a pure single frequency. They would appear on a spectrum analyzer as a single line as shown in **Figure 1**. Unfortunately, real signals are not pure tones. They appear to be phase modulated by noise. **Figure 2** is a more typical signal. The noise comes primarily from the active device in the oscillator. Its spectrum is shaped by the oscillator's resonator and the nature of the noise process. The noise process is beyond the scope of this paper but it is well documented in the literature **[1]**. Phase noise is specified by the ratio $\mathcal{L}(f)$. It is the noise power of one sideband in a one Hz bandwidth (power spectral density: W/Hz) offset from a carrier by a frequency, *f*, divided by the carrier power. The units are dB with respect to the carrier or dBc:

$$\mathcal{L}(f) = 10\log\left(\frac{P_{ssb}\text{ f from carrier in 1 Hz BW}}{P_{carrier}}\right)\text{ dBc}$$

An internet search will produce a wealth of information on phase noise measurement in application notes from Hewlett Packard (HP), Agilent, Keysight, Rohde & Schwarz (R&S) and others. A short introductory video by R&S can be found in **[2]**. The HP AN 283-3 **[3]** and the Hewlett Packard RF and Microwave Phase Noise Seminar **[4]** are very good. However, much of this material is written at a professional engineering level and it is often oriented toward the presenter's instruments. What is needed is something more oriented toward amateur needs.

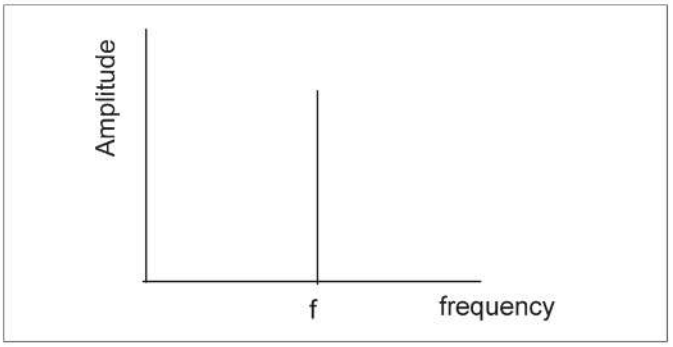

Figure 1 — An ideal signal appears as a single line on an ideal spectrum analyzer.

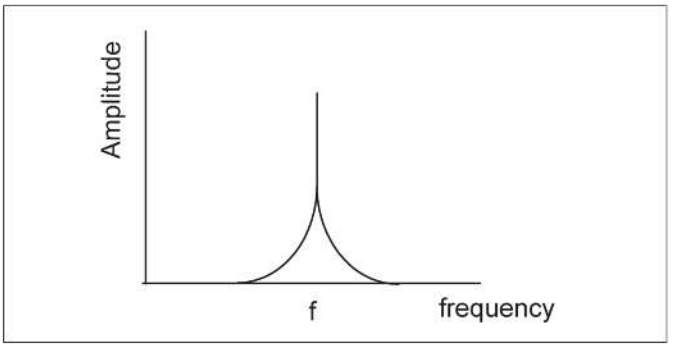

Figure 2 — A real signal with phase noise.

This paper is titled "revisited" because *QEX* and other amateur publications have published papers on phase noise measurement **[5] – [10]**. All of these papers provide useful insight but they really didn't provide the complete understanding that was needed to build a working system. In addition, performance had

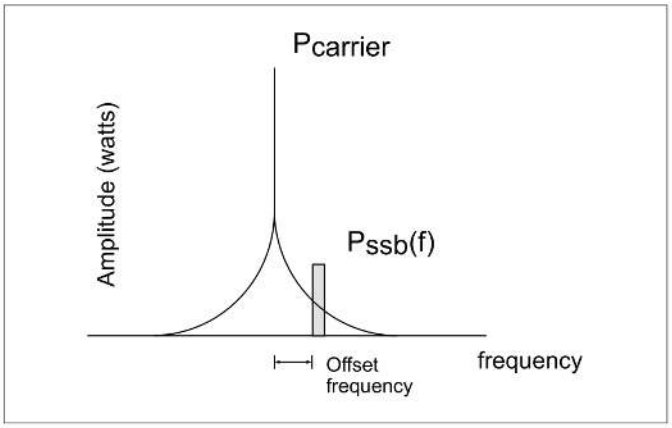

Figure 3 — Direct method of phase noise measurement. A narrow filter is used to measure the noise power at a frequency offset (Pssb(f)) from the carrier (Pcarrier).

to be verifiable and comparable to professional systems. Work to develop a phase noise measurement system was the result of a desire to evaluate the phase noise of crystal oscillators intended for microwave local oscillators **[11]**. It had to be capable of measuring very "quiet" sources in the 50 – 500 MHz range.

Direct Method of Phase Noise Measurement

The simplest method of measuring phase noise would be to measure the carrier power and then tune a one Hz wide bandpass filter to a frequency offset from the carrier by the desired amount and measure the noise power in that filter. **Figure 3** shows the direct method.

While intuitively satisfying, this is not so easy to do in practice. Measuring the phase noise of a 10 GHz signal at 10 kHz removed from the carrier would require a 1 Hz wide filter at 10.000010 GHz to measure the sideband noise power. Clearly, such a filter is not realizable. Narrow-band crystal filters have been used to measure phase noise but their utility is limited by available filter frequencies and bandwidths. Some filter measurement systems employ a heterodyne but that introduces the phase noise from an other oscillator **[12]**, **[13]**.

Modern spectrum analyzers can potentially do a direct measurement. Many analyzers have resolution bandwidths down to tens of Hz and it is possible to normalize the measured power by the resolution bandwidth to get watts per Hz (W/Hz). In addition, their phase lock tuning systems allow for very precise frequency settings.

A R&S FSEB spectrum analyzer with the low phase noise option and a Tektronix (Tek) 494P were used for direct phase noise measurement. Both analyzers have a GPIB interface which allows for computer control. With the right software it is possible to do phase noise measurement.

The utility of GPIB is often overlooked but the difficulty in using it is finding the interface hardware and the driver software. National Instruments makes a wide range of GPIB controllers. A GPIB to USB interface is available from Prologix but it is expensive at ~$300 **[14]**. Both the Prologix and a National Instruments GPIB-USB-HS interface were used to make computer controlled phase noise measurements.

While modern spectrum analyzers have become more available to amateurs, the phase noise measurement software is not as common. R&S provided software for the FSEB that did a direct phase noise measurement but it appears that software is no longer available. John Miles, KE5FX, has made his phase noise measurement software available for free download. It will create a phase noise measurement personality for a number of spectrum analyzers **[15]**. The FSEB and the Tek 494P as well as the Prologix GPIB interface are supported by the KE5FX software. The KE5FX website has a number of useful papers on phase noise measurement.

Ultimately, direct phase noise measurement is limited by the dynamic range of the spectrum analyzer. The minimum level or noise floor is set by the phase noise generated by the analyzer's own internal local oscillators. The noise floor in the FSEB is specified as −113 dBc at 10 kHz removed from the carrier for frequencies below 500 MHz. The Tek 494P, an older instrument, is 10 to 15 dB noisier. In addition, the noise floor is degraded as the frequency goes up because many spectrum analyzers, including the 494P, use harmonic mixing. Phase modulation theory requires that the noise floor increase by at least 20log(N) dB where N is the harmonic mixing number.

Figure 4 is the block diagram of a direct measurement system. The measurement is fairly straightforward. After establishing GPIB connectivity, the frequency and the power level of the test signal are specified in the KE5FX software. The desired minimum and maximum offset frequencies are specified. A "clipping" level is set along with the ratio of the video bandwidth (post detection) to resolution bandwidth. Clipping increases the spectrum analyzer sensitivity beyond the specified power level. This improves dynamic range, but use it prudently as setting the clipping too great can result in the spectrum analyzer being overloaded. For some spectrum analyzers, the post detection video bandwidth can be set independently of the resolution bandwidth. Narrowing the video bandwidth has the effect of averaging but it slows the measurement. The software also allows a correction for the detector noise response. This will be discussed later. A right click on an input box in the KE5FX software displays some helpful instructions.

The first measurement with the KE5FX software should be a noise floor test of the instrument being used. Check the spectrum

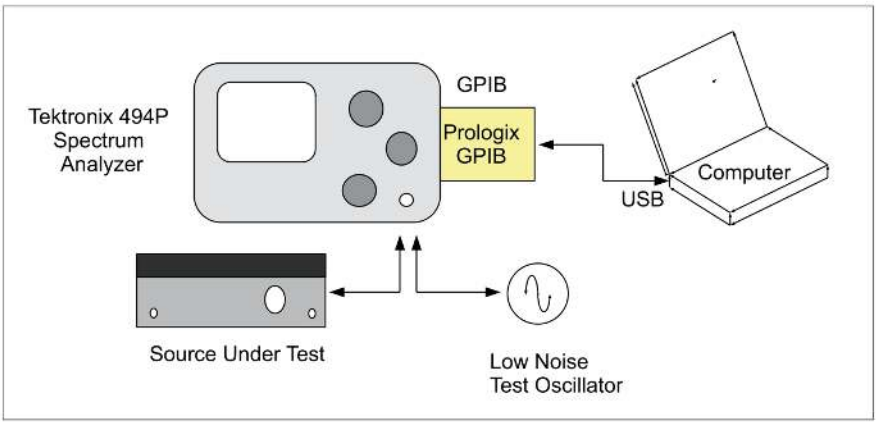

Figure 4 — System for direct measurement of phase noise using a spectrum analyzer.

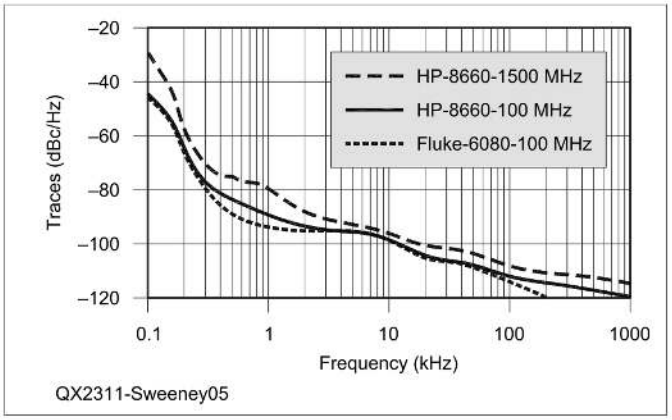

Figure 5 — This is the phase noise measurement of an HP8660C synthesizer using the KE5FX software and the Tek 494P. The HP8660C is an early synthesized signal generator and it is relatively noisy compared to many newer instruments.

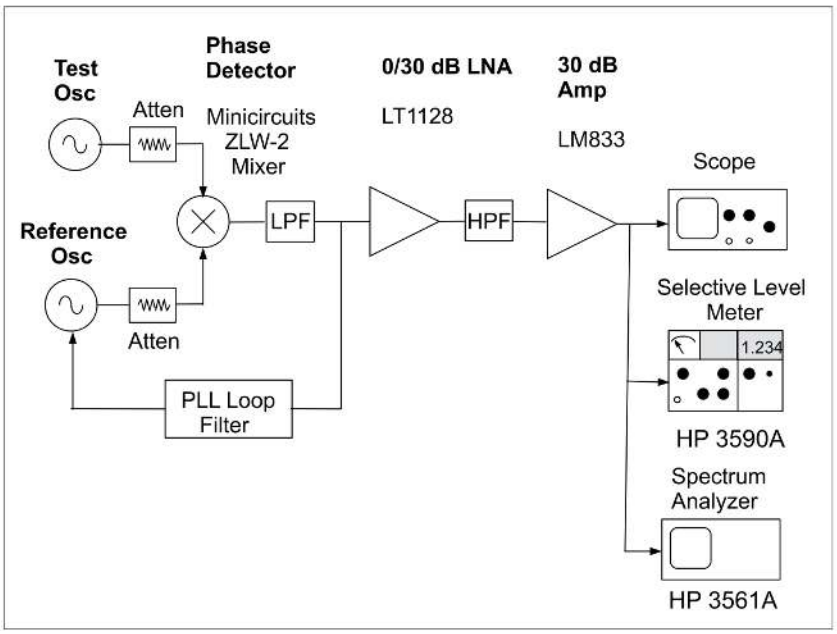

Figure 6 — PLL phase noise measurement system. (LNA: low noise amplifier, LPF: low pass filter, HPF: high pass filter).

analyzer manual for the specified noise floor. This test can be done by measuring the phase noise of a source known to have at least 10 dB lower noise than the measurement instrument. High quality Oven Controlled Crystal Oscillators (OCXOs) will probably challenge the phase noise measurement capability of most spectrum analyzers. The degradation of the noise floor can be a symptom of an aging instrument.

The HP8660C is an early synthesized signal generator and it is relatively noisy compared to many newer instruments. The lower dotted trace in **Figure 5** is the phase noise of a low-noise Fluke 6080A signal generator measured at 100 MHz. The 6080A has significantly lower noise than the 494P so this measurement represents the 494P's noise floor at 100 MHz. It is –97 to –98 dBc at 10 kHz offset from the carrier. This is approximately 15 dB worse than the more modern FSEB described above. The phase noise level at very low offset frequencies is questionable due to the limitation of the 30 Hz bandwidth resolution filter in the 494P.

The solid center trace in **Figure 5** is the phase noise of the HP8660C at 100 MHz. Where this trace merges with the lower trace, the measurement is being limited by the 494P. The upper dashed trace is the HP8660C at 1500 MHz. The 494P uses fundamental mixing at 1500 MHz so its noise floor can still be represented by the lower trace measured at 100 MHz. The HP8660C requires an additional doubler to reach 1500 MHz so its phase noise will increase by at least 6 dB over its noise at 100 MHz. That can be seen in the upper dashed trace.

Phase Noise Measurement using a PLL and a Phase Detector

The direct method is relatively easy but it is limited by the phase noise performance of the spectrum analyzer. A significantly more sensitive measurement employs a PLL with a phase detector and a low frequency spectrum analyzer. **Figure 6** is a block diagram of the PLL phase noise measurement system. The effect of the PLL is to translate the carrier frequency down to zero. Notice the similarity to a direct conversion receiver. Many of the techniques for building a good direct conversion receiver apply here. This system was patterned after the one described by Wenzel Associates **[16]**.

Phase Detector and PLL

A double balanced diode ring mixer (DBM) is used as a phase detector. With this phase detector, a PLL will hold the test and reference signal in phase quadrature, i.e., 90° out of phase. The phase detector output is a voltage proportional to the phase difference from the 90° between the test and reference signals. With phase quadrature, the amplitude noise of the signal tends to be suppressed by the phase detector. Its output is due to the phase differences alone. The direct spectrum analyzer method measures a combination of phase and amplitude noise. Amplitude noise tends to be less prominent than phase noise in well designed oscillators.

Inside the loop bandwidth, the two signals track in phase and the phase difference is driven toward zero. Outside the loop bandwidth both signals contribute to the phase difference so the power spectral density of the output represents the combined phase noise power of the two signals. **Figure 7** shows the spectrum of the phase detector output. The performance of this system is limited by the phase noise of the reference signal.

The PLL bandwidth should be set so it is much less than the minimum desired offset frequency. A factor of 10 is a good place to start. To measure phase noise 100 Hz from the carrier, the PLL bandwidth should be 10 Hz or less. However, there is a trade-off. Depending on the stability of the oscillators, it may be difficult to obtain and maintain phase lock with very narrow loop bandwidths.

Passive diode ring mixers are ideal phase detectors but it is important to understand their limitations. They must be used properly in order to realize their full potential **[17]**. An important

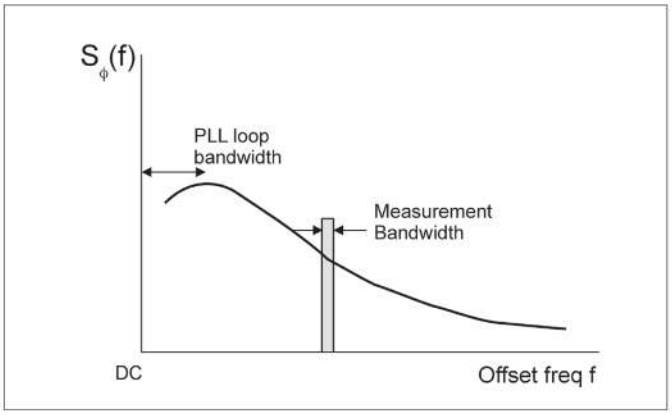

Figure 7 — The spectrum of the phase power spectral density at the output of the phase detector.

consideration is the DBM IF port must work down to DC. One potential source of error is the frequency response of the IF port. It may not be flat with offset frequency. A pair of signal generators calibrated in level and frequency can be used to test this. Set one generator as the LO with the correct power level for the DBM and other as the RF with the correct level. The IF port should be terminated as a phase detector. Observe the difference frequency or beat note on the IF port with an oscilloscope or a spectrum analyzer as the generators are tuned apart. The output level should remain constant as the beat note frequency changes. The phase noise box described later can be set up to do this test.

A Minicircuits ZLW-2 DBM (an obsolete part from my junk box) was used as the phase detector. Choose a DBM with high LO-RF isolation and all three ports should be properly terminated. The attenuators in **Figure 6** ensure proper termination and tend to improve isolation. Most DBMs have better isolation at the lower end of their specified frequency range. A DC offset voltage, i.e., a non-zero output voltage for the 90° phase difference, is inherent in all DBMs and it is related to internal balance and port isolation **[18]**. This offset may result in phase lock at a phase angle different from 90°. The resulting error is 20log(cosine of the offset angle from quadrature). With a high quality DBM, this error should be small.

Measurement Analysis

The test and the reference signals are applied to the phase detector. It acts as a multiplier and its output is the sum and difference of the applied signals. Since the PLL holds the test and reference signals at the same frequency and 90° out of phase, the difference output is a DC signal that is proportional to the sine of the phase difference between the signals. Given the phase lock, the radian frequency $\omega = 2\pi f_{carrier}$ of the two signals is equal so the sum output frequency is 2ω. The output of the phase detector is given by:

$$\begin{aligned} V_o &= \mathrm{K}\left[V_{\text{tcst}}\sin\left(\omega t+\varphi_1\right)\right]\left[V_{\text{ref}}\cos\left(\omega t+\varphi_2\right)\right] \\ &= \mathrm{K}_\varphi\left[\sin\left(\varphi_1+\varphi_2\right)+\sin\left(2\omega t+\varphi_1+\varphi_2\right)\right] \end{aligned}$$

K_φ is the phase detector gain constant and $\left(\varphi_1+\varphi_2\right)$ is the phase difference between the two signals. Notice that the signal amplitudes and the ½ factor in the trig expansion for the multiplication are absorbed into K_φ which will be measured later. A simple type 2 second order loop with an op amp integrator tends to drive the phase difference towards zero inside the loop bandwidth. The low pass filter in **Figure 6** removes the twice frequency component, and, if the phase difference $\left(\varphi_1-\varphi_2\right)=\Delta\varphi$ is small, the sine can be approximated by its argument:

$$V_o = K_\varphi \sin\left(\Delta\varphi\right) \approx K_\varphi \Delta\varphi$$

Typically the difference is assumed to be less than 0.1 to 0.2 radians for this approximation to hold. **[19]** Now, the difference voltage outside the loop bandwidth is measured in a narrow filter set for the desired offset frequency. Since the output is centered around zero frequency, the measurement can be done with a low frequency spectrum analyzer. This measurement results in a voltage that is proportional to phase noise spectrum at the desired offset frequency *f* in the measurement bandwidth:

$$V_{\text{orms}}\left(f\right) = K_\varphi \Delta\varphi_{\text{rms}}\left(f\right)$$

In order to calculate noise power, V_o is measured as an rms voltage. The bandwidth (BW) of the measurement system should be relatively narrow with respect to the offset frequency so the noise power can be assumed to be constant over the measurement bandwidth. The voltage measurement is squared to calculate power and this is normalized by the measurement BW. The result is the phase power spectral density:

$$S_\varphi\left(f\right) = \frac{\Delta\varphi^2_{\text{rms}}\left(f\right)}{\text{BW}} = \frac{V^2_{\text{orms}}\left(f\right)}{K^2_\varphi \text{BW}} \quad \frac{\text{rad}^2}{\text{Hz}}.$$

By applying phase modulation theory, it can be shown that $S_\varphi\left(f\right)$ and $\mathcal{L}\left(f\right)$ are related by:

$$\mathcal{L}\left(f\right) = \frac{S_\varphi\left(f\right)}{2} = \frac{P_{\text{ssb}}\left(f\right)}{P_{\text{carrier}}}$$

The rms voltage of the phase noise at the offset frequency *f* has been measured and the bandwidth of the measurement system is known so it is possible to calculate $\mathcal{L}\left(f\right)$:

$$\mathcal{L}\left(f\right) = \frac{V^2_{\text{orms}}\left(f\right)}{2K^2_\varphi \text{BW}}$$

The phase detector sensitivity K_φ is unknown but it can be measured. The technique is to open the PLL and offset the test and reference signal by a few hundred Hz or a kHz or two. The phase detector now outputs a difference or beat frequency. This signal can be used to determine K_φ which is the slope or the derivative of the output signal evaluated at zero phase error:

$$\begin{aligned} K_\varphi &= \frac{\mathrm{dV}_o}{\mathrm{d}\Delta\varphi} = \frac{d\left(V_{\text{bpk}}\sin\left(\Delta\varphi\right)\right)}{\mathrm{d}\Delta\varphi} = V_{\text{bpk}}\cos\left(\Delta\varphi\right) \\ &= V_{\text{bpk}};\ \text{where}\ \left(\Delta\varphi\right)=0 \end{aligned}$$

V_{bpk} is the peak voltage of the beat frequency signal. K_φ is simply the peak voltage of the beat frequency. It can be measured with the same spectrum analyzer that is used to measure the noise voltage at the offset frequency. K_φ can also be mea-

sured with an oscilloscope by measuring V_{bpk} or by measuring ΔV for a Δt at the zero voltage crossing and calculating:

$$K_\varphi = \Delta V / \Delta t \ .$$

The ΔV, Δt measurement is a different measurement from the V_{bpk}. Since the amplitudes of the applied signals are contained in the K_φ measurement, it establishes the carrier power level.

There are two important caveats for using this measurement to obtain K_φ. The first is this measurement must be made under the same operating conditions that the noise voltage measurement at the offset frequency is made. The power levels applied to the phase detector must be the same for both measurements. This is no small task due to the large difference in output level between these two measurements. The gain of the LNA in the phase noise box can be changed while maintaining the operating conditions by changing the LNA's feedback network. The gain of the LNA can be set to either 0 dB or 30 dB and a second amplifier is available for an additional switchable 0 dB or 30 dB gain. The LNA remains connected to the mixer and, at the lower gain, the amplifiers remain in their linear range for the stronger beat frequency signal.

The second requirement is that the output signal should be sinusoidal. Running the DBM phase detector at high levels increases system sensitivity but that potentially pushes it into a nonlinear range. It is desirable to run the DBM in its saturated mode **[20]** where the output voltage is relatively insensitive to the applied level, however, deep in the saturated mode, the output waveform becomes more triangular rather than sinusoidal. Observe the harmonics of the of the beat signal with the spectrum analyzer. The ZLW-2 operates with a 10 dBm LO input and a 0 dBm RF input. Depending on the applied signal level, the worst case harmonic tends to be the 3rd harmonic. If it is 25 to 30 dB below the beat note signal that should be adequate for a sinusoidal signal. The balanced nature of the DBM tends to suppress the even order products. The output of the ZLW-2 DBM under the beat frequency test condition is approximately 0.16 V peak. This results in $K_\varphi = 0.16$ volts per radian.

Finally, note when to use the rms and peak voltages. The beat note is measured as an rms voltage so a factor of $\sqrt{2}$ is needed for the calculation of K_φ. The noise voltage at the desired offset frequency is measured as rms and the bandwidth of the measurement system is known. It is now possible to calculate $\mathcal{L}(f)$ from the measurements:

$$\mathcal{L}(f) = \frac{V_{\text{orms}}^2(f)}{2\left(K_\varphi\right)^2 \text{BW}} = \frac{V_{\text{orms}}^2(f)}{2\left(\sqrt{2}V_{\text{brms}}\right)^2 \text{BW}} = \frac{V_{\text{orms}}^2(f)}{4V_{\text{brms}}^2 \text{BW}}$$

In decibels:

$$\mathcal{L}_{dB}(f) = 20\log\left(V_{\text{orms}}(f)\right) - 20\log\left(V_{brms}\right) - 10\log(\text{BW}) - 6 \pm \text{Corrections dBc}$$

There are several corrections that may be needed to accommodate the measurement technique and the equipment used:

- Noise bandwidth: $-10\log\left(\text{BW}_n/\text{BW}_{3\text{dB}}\right)$.
- System gain: 0, –30, –60 dB.
- Detector type: +2.5 dB for log amp/peak detector; 1.05 dB peak responding, rms calibrated.
- Contribution of reference oscillator: –3 dB if oscillators are identical.
- Averaging.

Noise Bandwidth:

The noise bandwidth is the bandwidth of an ideal square sided filter that admits the same noise power as the real filter in the measurement system. The real filter is the resolution bandwidth filter in the spectrum analyzer and, in swept frequency spectrum analyzers, it often has a Gaussian shape. Depending on the filter shape and the number of resonators, the noise bandwidth is usually somewhat more than the 3 dB filter bandwidth. Generally this is a small correction, less than ±1 dB, but it can become more complex with an instrument that uses the Fast Fourier Transform (FFT) to do the filtering. Consult the user manual of the spectrum analyzer.

System Gain

The noise voltage measured after phase lock has been established is tiny and measurement requires significant additional gain. With the phase noise box, the gain can be set for 0 dB, 30 dB or 60 dB. The 60 dB gain is used for very quiet oscillators. The $\mathcal{L}(f)$ measurement requires that the phase noise voltage be compared to the beat frequency voltage at the output of the phase detector. This means that any additional gain must be accurately determined and subtracted out before $\mathcal{L}(f)$ can be calculated. The K_φ measurement is a high level measurement and it is usually done at 0 dB gain. With very quiet oscillators, the noise measurement maybe up to 100 dB below the beat frequency voltage so even with 60 dB of gain the spectrum analyzer will need 40 dB or more dynamic range. Be aware of the dynamic range and noise floor of the spectrum analyzer. Early work with an USB FFT based spectrum analyzer produced inconsistent results because its 8 bit A/D had inadequate dynamic range.

Detector Type

The log amp/peak responding detectors in many spectrum analyzers respond differently to noise than they do to sinusoidal CW signals. Due to the statistical nature of noise, a log amp/peak responding detector will read 2.5 dB low when measuring noise, thus the need to add 2.5 dB. Similarly 1.05 dB must be added for the peak responding, rms calibrated detectors used in many wide-band AC voltmeters and selective level meters. Some spectrum analyzers have true rms detectors and do not need the correction. The KE5FX software allows for the specification of a detector noise correction. A +2 dB correction was applied to the Tek 494P measurement above. Again, check the user manual for the spectrum analyzer's detector.

Reference Oscillator

Voltage variable crystal oscillators (VCXOs) and low phase noise signal generators with DC coupled frequency modulation capability are potential reference sources. See **[21]** for a discussion of the correction for the noise contribution from the reference oscillator. It can be safely ignored if the reference has 10 dB or lower phase noise than the test oscillator. If the two

oscillators are identical, it can be assumed that they contribute equal phase noise and the resulting measurement can be reduced by 3 dB to obtain the phase noise of the test oscillator. It is also possible to measure pair-wise three different oscillators and then use the "three cornered hat" analysis described in **[22]** to obtain the phase noise performance of each source.

Averaging

Many modern spectrum analyzers have an averaging function that improves the accuracy of noise measurements. Averaging 30 measurements reduces the uncertainly window to −1.3 dB to +1.8 dB for a 95% confidence level. See **[23]** for an analysis on the effect of averaging. In the absence of an averaging function, reducing the post detection video bandwidth has the effect of averaging. Without averaging, it may be difficult to determine the noise level due to the variability of the measurement.

Low Frequency Spectrum Analyzers

An important part of any phase noise measurement is the spectrum analyzer. Many microwave spectrum analyzers will go down to 100 kHz or even 10 kHz but they tend to be too noisy at this low frequency for phase noise measurements.

Selective level meters (SLM) or wave analyzers can be used as low frequency spectrum analyzers. SLMs are tunable calibrated low frequency receivers with selectable bandwidths. Early measurements were made with an HP3590A/3594A SLM. It tunes from 20 Hz to 620 kHz, has an 80+ dB dynamic range and available 10, 100, 1000 and 3100 Hz bandwidths. Its detector is peak responding, rms calibrated. To improve noise measurement, it was modified to increase its post detection analog averaging. The HP3581 and HP3586 are similar instruments that are newer. The disadvantage of the SLM is that its manual tuning allows only a point by point measurement. Given that SLMs are now obsolete, they have gotten expensive and somewhat hard to find. The SLM used was a $5 Hamfest find.

There are a number of low frequency spectrum analyzers that should work. The HP3563 (100 kHz), HP3582 (25 kHz) and the HP3585 (40 MHz) are described in various HP app notes on phase noise measurement. Phase noise measurement with the HP3585 is described in **[24]**.

Dynamic signal analyzers are FFT based spectrum analyzers. An HP3561A dynamic signal analyzer was used for many of the tests in this paper. It measures up to 100 kHz and has an 80 dB dynamic range. It does rms measurements and averaging. In fact, the HP3561A was used in the HP3048 phase noise measurement system but it too is obsolete, and the few that are available have gotten expensive. The instrument was purchased from an auction site for about $350. The HP 3562 and 3563 are newer dynamic signal analyzers.

High end audio sound cards with 16 or 24 bit A/Ds are a possibility if the right kind of spectrum analyzer software can be found. A sound card spectrum analyzer program was investigated but its resolution bandwidth could not be determined so its noise bandwidth is unknown. Software should be able to do averaging and to output the noise bandwidth of the measurement or power spectral density (W/Hz). The search for the right software continues.

A number of inexpensive USB scopes have FFT spectrum analyzer functions. Most are limited by their 8 bit A/D and their dynamic range is inadequate. The FFT spectrum analyzer in the Velleman pcsgu250 was tried. It could report power spectral density but it lacked the needed dynamic range. The Digilent Analog Discovery 2 has a FTT spectrum analyzer with a 14 bit A/D. It will do averages, rms measurement, and reports noise bandwidth **[25]**. While it should have adequate dynamic range, tests with the Analog Discovery and the HP3561A did not agree. It is speculated that the noise measurements were too close to the Analog Discovery's noise floor. Careful gain management may help overcome dynamic range limitations but there is more work to be done.

An active filter after the LNA is an analog solution **[26]** but each filter is limited to a single offset frequency. It is relatively easy to build active filters with a specified gain, bandwidth and center frequency **[27]**.

For an analog system, the amplitude detector after the amplifier and the filter can be a wideband AC voltmeter such as an HP400 (peak responding, rms calibrated) or an rms responding instrument such as an HP3400. Depending on the system gain, the detector needs to operate to the millivolt level. In addition, the frequency response of many inexpensive digital voltmeters is limited and some so called "true" rms meters do not handle noise well. They calculate rms mathematically but their ability to handle large crest factors is limited. **[28]** Crest factor is the ratio of the peak value to the rms value of a waveform. Theoretically Gaussian (white) noise has an infinite crest factor but in practice it is much less. The HP3400 responds well to noise as it measures rms thermally and can handle a crest factor of up to 10.

The Phase Noise Box

Figure 8 is the circuit schematic for the phase noise box used to support the noise measurement system. **Figure 9** is a picture of the phase noise box. It has two parts: a wide-band high-gain low-noise amplifier and an active PLL loop filter. The high- gain amplifier is implemented with low-noise op amps. Op amps have both an internal noise voltage and an internal noise current. Since the output impedance of the phase detector is low, it is important to choose a low voltage noise op amp for the phase noise box LNA. An in-depth discussion of noise in op amps can be found in **[29]**. There are a number of low voltage noise op amps and, in the course of development, several were tried. In rough order of decreasing performance (and cost), the LT1128, AD797, LM4526, NE5534 (requires additional compensation for unity gain), NE5532 or LM833 are usable. They are all capable of driving the relatively low resistance feedback network needed to reduce the effect of resistor noise. They must be capable of operating as unity gain amplifiers as the LNA can be set for 0 dB or 30 dB gain. Although it is relatively expensive (~$18), the LT1128 was chosen for its low noise performance. There may be other amps. The "lowamp" reference in **[16]** is a discrete component amp with potentially better performance. Be cautious of things obtained from the internet. An AD797 obtained from an auction site turned out to have a questionable pedigree as the measured noise far exceeded that specified in the data sheet.

It is possible to select 0 dB, 30 dB, or 60 dB gain in the phase noise box. In the 60 dB gain mode, the amplifier frequency response is down less than 1 dB at 100 kHz. Measurements to 100 kHz offset are possible. The resistors in the feedback path are 1% metal film to reduce excess resistor noise and to ensure accurate gain. The SMA input from the phase detector has a chip

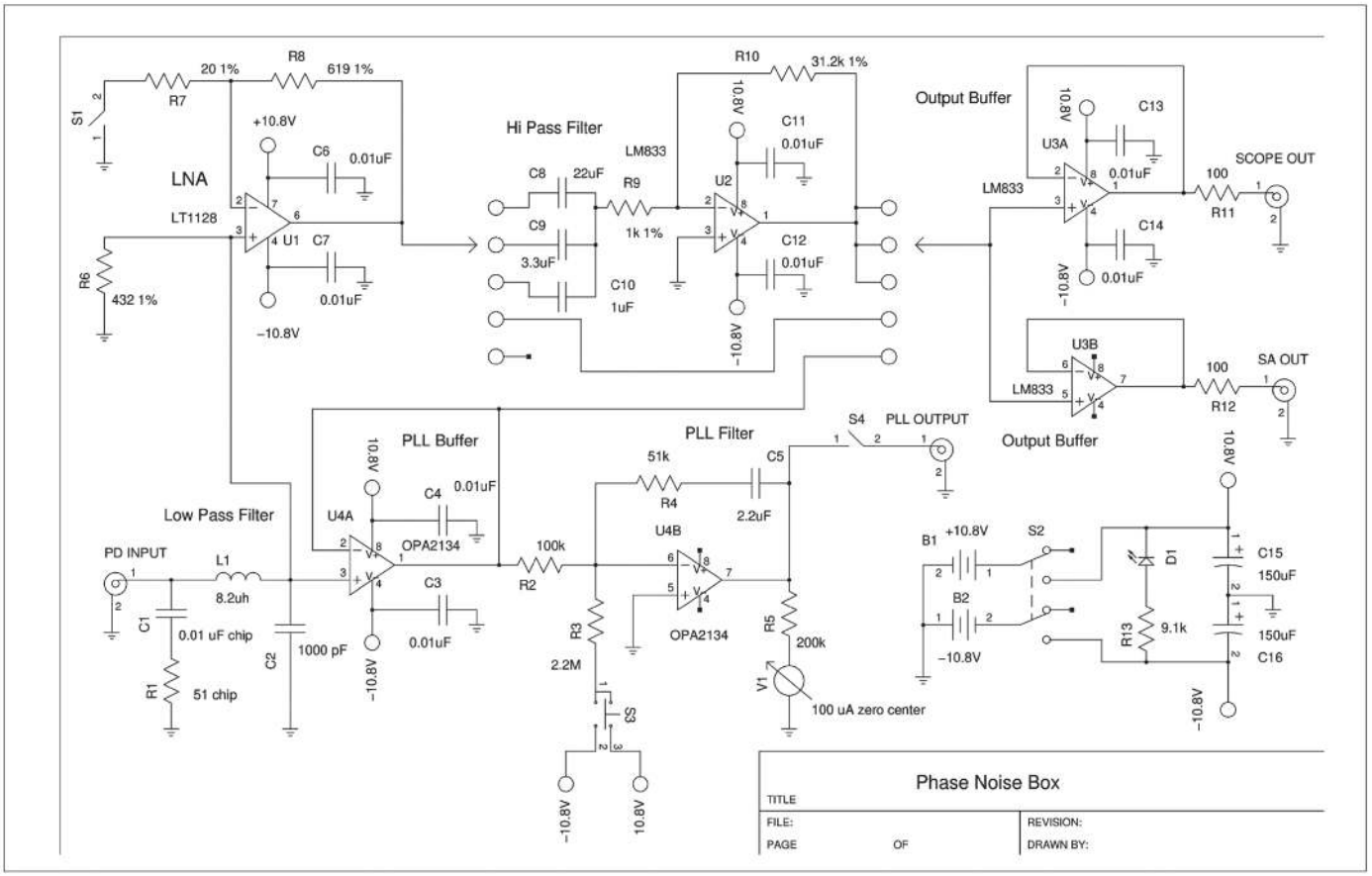

Figure 8 — Phase noise box circuit.

Figure 9 — Phase noise box with DBM. The insulated bushings on the left are tie points for the PLL loop resistors, R2 and R4 in Figure 8.

capacitor and chip 51 Ω resistor in series to ground. This terminates the phase detector output at high frequencies. There is also a simple *LC* low pass filter (L1, C2) to remove the twice frequency component of the phase detector output.

Selectable AC coupling forms a simple high pass filter. This blocks any DC offset from the DBM. C8, C9 and C10 in **Figure 8** set the 3 dB high pass frequency to 7 Hz, 48 Hz or 159 Hz respectively. The high pass amplifier is a LM833 with a gain of 30 dB. It can be bypassed with the selector switch in the center of the schematic. The switch can also route a 0 dB or 30 dB DC response to the output. S1 sets the LNA gain to 0 dB or 30 dB.

LM833s are used as output buffers. They were probably not the best choice. Due to their high gain-bandwidth product, they become unstable when driving capacitive loads such as a length of coax cable terminated in a high impedance like an oscilloscope. It was necessary to add 100 Ω resistors in series with their outputs to insure stability. Since the buffers have a gain of 1 and low-noise performance is not needed, a lower gain-bandwidth product op amp that can support unity gain to 100 kHz should work.

The PLL circuit uses a unity gain buffer amp so the loop filter and the phase detector see a constant source and load impedance. The original design used a dual LF353 FET op amp for its low current noise. Since the PLL filter is a high impedance circuit, low current noise is more important than low voltage noise thus the choice of a FET input op amp. The LF353 was later replaced with the FET input OPA2134 that has even lower current noise and also relatively low voltage noise. It is more expensive (~$6). Given the relatively low voltage noise of the OPA2134, the gain of the buffer could be increased to accommodate low sensitivity VCXOs. While not optimized for DC, the OPA2134 has a somewhat lower input offset voltage than the LF353. This reduces open loop drift in the PLL integrator. The gain of the PLL filter tends to decrease with increasing frequency so the noise tends to be attenuated but it is important to keep in mind that the noise

output from the PLL circuit phase modulates the reference oscillator.

An additional circuit with a center-off SPDT switch (S3 and R3 in **Figure 8**) is used to introduce an offset current that will sweep the PLL output voltage up and down to facilitate phase locking. The zero-center meter on the PLL output is used as a tuning aid and a DC coupled output observed with an oscilloscope can also aid in phase locking. Probably the best phase lock aid is observing the beat note on the HP3561A in real time as the loop pulls in to phase lock. S4 in **Figure 8** allows opening the PLL.

The phase noise voltage measurement falls in the millivolt range and that is after 60 dB of gain! Careful shielding is required. The circuitry is built into a shielded box. It is powered by rechargeable batteries to reduce the effect of power supply noise, ground loops and coupling from external sources. The high gain of the LNA makes this particularly important as spurious 60 Hz spectral lines show up if the box gets too close to just about anything that is mains powered.

The test and reference oscillators must be carefully shielded and isolated to reduce the potential of cross coupling or injection locking. Injection locking occurs when the two oscillators can influence one another. It can be subtle and it will usually result in unrealistically low phase noise measurements. Poor DBM isolation, power supply cross coupling, poorly shielded oscillators and inadequate buffering can all contribute to injection locking. Much of the system testing was done with high performance signal generators that were well isolated and shielded. Shielded connectorized DBMs are desirable as are high quality double-shielded cables. Having oscillators just sitting open on the bench next to each other is almost a guarantee of degraded performance. If moving things around on the bench causes significant changes to the measurement, that is potentially a sign of undesired coupling.

Example

Two identical Bliley NV26R891 100 MHz OCXOs were used as the test and the reference oscillators. These are very low phase noise sources with a voltage tuning port. Their output is 7 dBm. One oscillator was fixed tuned to 100 MHz and the other was used as the reference Voltage Controlled Oscillator (VCO) in the PLL. The phase detector was the ZLW-2 with 7 dBm from one oscillator applied directly to the LO port. The RF port was set at –3 dBm from the other oscillator with a 10 dB attenuator.

Test procedure

- Open the PLL and set both amplifiers in the phase noise box for 0 dB gain.
- Apply the correct levels to the LO and RF ports of the DBM.
- Offset the reference and the test oscillator frequency.
- Display the beat note on the spectrum analyzer and check for linear operation.
- If the system is linear, measure and record the amplitude of the beat note, use the rms value for the phase noise calculation, the peak value for K_{φ}.
- Calculate and apply the desired PLL loop parameters, ω_n and ζ.
- Close the PLL and phase lock the reference and test oscillators.
- Choose 30 or 60 dB gain and the desired high pass frequency.
- Measure the noise voltage at the desired offset frequency with the spectrum analyzer using averaging.
- Record the measurement BW.
- Apply the corrections and calculate $\mathcal{L}(f)$.

Figures 10 and **11** show the noise measurements using the HP3561A dynamic signal analyzer. The 3561 reports voltage as dB with respect to a volt, dBV.

V_{brms} = –19.14 dBV; Measurement BW = 19.097 Hz; High pass = 48 Hz.

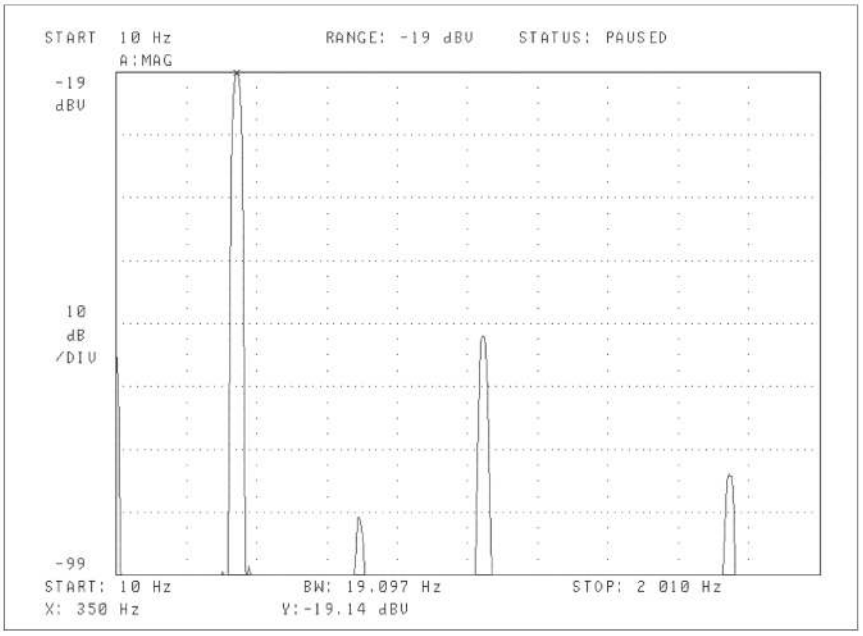

Figure 10 — Beat note measurement, PLL unlocked: Vbrms = –19.14 dBV at 350 Hz. The measured BW is 19.097 Hz. The third harmonic is more than 40 dB below the fundamental so the output is sinusoidal. Gain is 0 dB.

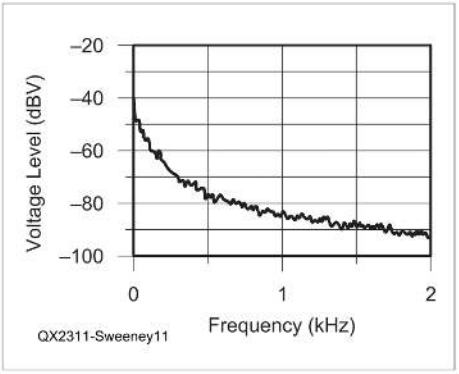

Figure 11 — Noise measurement after phase lock. Vorms(1 kHz) = –85.18 dBV. The plot is an average of 30 rms measurements. Gain is 60 dB.

The measured phase noise after an average of 30 measurements is –85.18 dBV at 1 kHz offset with 60 dB of gain. The oscillators were assumed to be identical. No correction was made for noise bandwidth or detector type as the HP3561A does an rms measurement.

$$\mathcal{L}(f) = 20\log\left(V_{\text{orms}}(f)\right) - 20\log\left(V_{brms}\right) - 10\log(\text{BW}) - 6 \pm \text{Corrections dB}$$

$$\mathcal{L}(f) = -85.18\ \text{dBV} - (-19.14\ \text{dBV}) - 10\log(19.097\ \text{Hz}) - 6 - 60 - 3 = -147.8\ \text{dBc}$$

This value is consistent with the published spec for the Bliley oscillator. The measured and specified phase noise are plotted in **Figure 12**. With the –3 dBm test signal, –161 dBc represents the noise floor in the system.

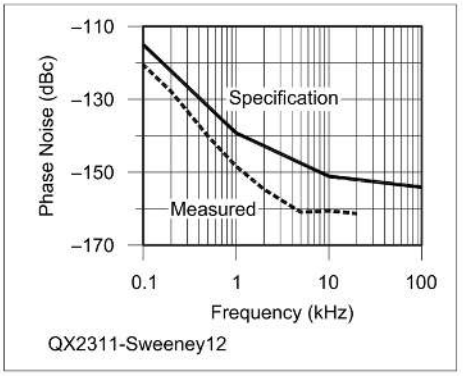

Figure 12 — Bliley NV26R891 100 MHz OCXO phase noise. The upper trace is the published phase noise spec and the lower trace is the measured phase noise.

Verification

Figure 13 shows the phase noise measurement made with a pair of HP8640 and Fluke 6080A signal generators. The HP has a free running master oscillator and the Fluke is a synthesizer. The upper dotted line in **Figure 13** is the 6080A phase noise specification at 10 MHz. The solid trace is the measured noise of the 6080A at 10 MHz. The dash-dot line is the 8640 at 10 MHz. The 8640 is especially good because it divides its fundamental 256 – 512 MHz oscillator by 32 to reach 10 MHz. Each divide by 2 theoretically reduces the phase noise by 6 dB. The –150 dBc noise floor of the 8640 is probably due to the residual noise in its dividers. The dashed trace is the 8640 at 100 MHz. The 8640 starts to get noisy at less than 1 kHz offset and the increasing phase noise with decreasing offset is evident.

While the exact value of the measured phase noise could not be verified, the signal generator measurement and the measurement of the Bliley low-noise 100 MHz OCXOs agreed well with the published phase noise specs for these sources.

A 53.85 MHz crystal oscillator designed for a microwave LO was measured at the 2023 Microwave Update conference with a R&S FSWP Phase Noise Analyzer. The FSWP is a state-of-the-art digital cross correlation analyzer. The FSWP measured the oscillator at –145.3 dBc at 1 kHz. The same oscillator measured –146.4 dBc at 1 kHz with the system described here.

The system noise floor determines the lowest possible level that is measurable but determining the noise floor can be challenging. The required dynamic range makes this a difficult measurement to make. The noise floor can be measured by splitting a test signal with a 3 dB 90 degree power splitter and adjusting the levels for the DBM with the appropriate attenuators. Since the noise in both legs comes from the same source, it is correlated. When this test signal is multiplied in the phase detector, the difference is taken. The result is the test signal noise is canceled leaving the residual noise in the system.

Phase detector balance determines how well the source phase noise is suppressed. About 20 to 30 dB is probably reasonable so to get to the noise floor a low phase noise source is required. A 10 MHz OCXO was used as a test source. The test signal was split with the 90° hybrid shown in **Figure 14**. Assuming that the offset voltage is small, exact quadrature can be obtained by monitoring the DC voltage out of the phase detector and adjusting C3 on the hybrid for zero voltage. The 30 dB DC coupled amplifier function in the phase noise box was used to increase the sensitivity of this measurement. The test source was built into a shielded enclosure and operated from a battery but even then there was some 60 Hz interference. It helped to turn off all the nearby test equipment, soldering iron, desk lamp, etc.

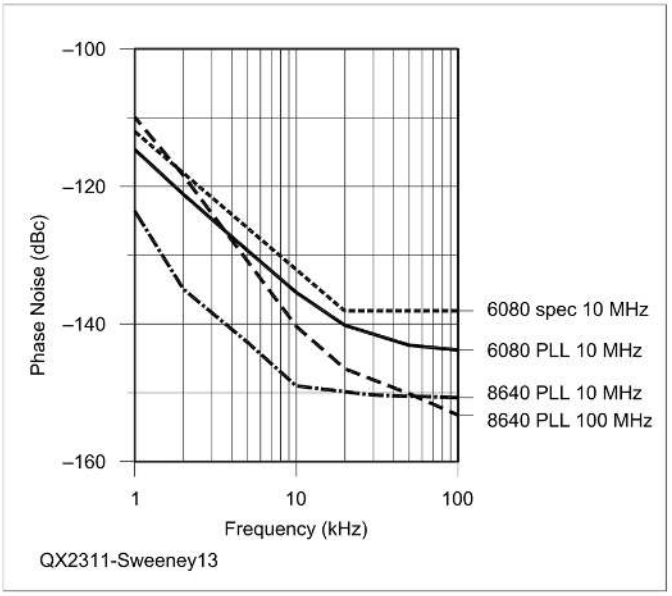

Figure 13 — Phase noise measurement of the HP8640 and the Fluke 6080A signal generators.

The phase detector was calibrated with two Fluke 6080A signal generators. One generator was set to 10 MHz and the other was set for an offset of a few hundred Hz. The power levels were set to the same level as the test source. These two signals were used to determine the phase detector K_{φ}. The quadrature signals from the test source were then applied to the phase detector. There is no phase lock but the phase noise measurement at the desired offset was made with the spectrum analyzer and $\mathcal{L}(f)$ was calculated with this measurement. The result is the noise floor at the chosen offset frequency.

The limitation appears to be the DBM. Most of the measure-

ments were made with the ZLW-2 with 10 dBm for the LO and approximately 0 dBm on the signal port. With a 0 dBm test signal, the measured noise floor is approximately −165 dBc at 1 kHz. The measurement shown in **Figure 12** was done with −3 dBm on the RF port of the DBM. The noise floor is approximately −161 dBc at that signal level.

Given the noise parameters of the op amp and the thermal noise of the resistors, it is possible to calculate the noise output. The LNA input was terminated with 50 Ω and an on-line calculator **[30]** was used to calculate the noise output. With $T = 300$ K, BW = 19.097 Hz and gain = 60 dB, the calculated output was −104.4 dBV. The actual output noise was measured with the HP3561A. The measured and calculated noise agreed within 1 dB.

The dynamic range (*DR*) can be estimated from the applied test signal, the conversion loss in the DBM, the LNA noise figure (*LnaNF*) and the thermal noise floor. The thermal noise floor is −174 dBm/Hz. (Thermal noise floor = kT = Boltzmann's constant times the Kelvin temperature 300 K) The *LnaNF* was estimated with the calculator in **[30]**:

$$\begin{aligned} DR &= (testsignal) - (DBMloss) - (LnaNF + NoiseFloor) \\ &= 0 \text{ dBm} - 6.0 \text{ dB} - (4.5 \text{ dB} - 174 \text{ dBm/Hz}) \\ &= 163.5 \text{ dB} \end{aligned}$$

The accuracy of the DBM loss is open to question because it is being used as a phase detector rather than as a mixer, however the estimate is consistent with the measured −165 dBc. This analysis does not account for the 1/*f* noise in the op amp that increases the LNA noise figure at lower offset frequencies. The practical lower limit is defined by the LNA noise figure and the −174 dBm/Hz thermal noise floor. A higher level test signal should improve dynamic range. A higher level ZLW-2H DBM was available but the power available from the test source would not support the ZLW-2H.

Conclusion

This paper covers experience with two types of phase noise measurement. The direct spectrum analyzer method is relatively straight forward. If a modern low phase noise spectrum analyzer with GPIB is available and it is supported by the KE5FX software, it is worth a try. The spectrum analyzer's noise floor limits the dynamic range so it is good to measure a low-noise source so the noise floor is known.

The PLL based phase noise measurement is more complex but it is capable of much higher performance. It requires a low phase noise reference source and a number of the very low noise measurements were made using identical oscillators. Because of its sensitivity, it is subject to 60 Hz interference. Care must be exercised in order to get meaningful results with this technique but it is not beyond the capability of committed amateurs. It is hoped this paper will provide the basis for others to develop the capability of doing phase noise measurements.

Most of the major sources of error for phase detector/PLL system have been noted:

- Accuracy of the beat note measurement.
- Spectrum analyzer amplitude accuracy.
- Phase detector flatness.
- Sinusoidal output.

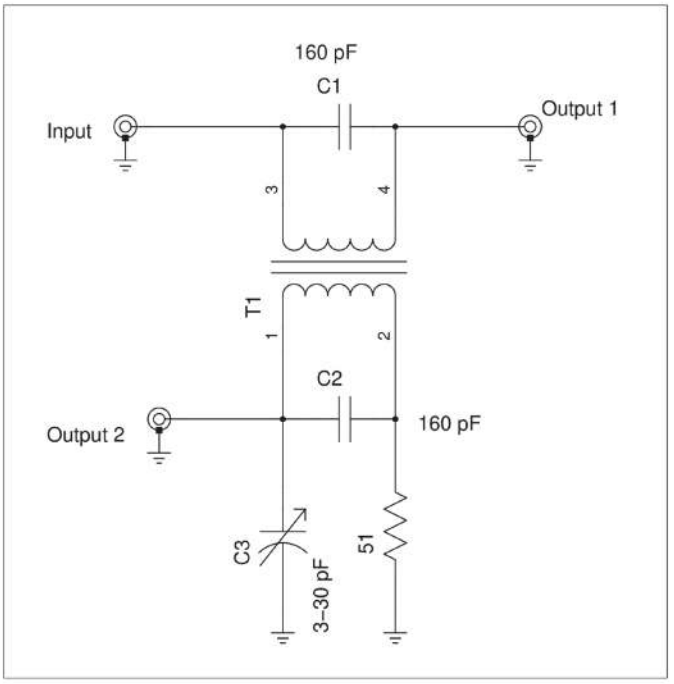

Figure 14 — 10 MHz 90° phase splitter. T1 is18 turns of bifilar wound #30 AWG wire on a T25-2 core. C3 is used to adjust the exact quadrature. It can be attached to either output 1 or output 2 and adjusted for best quadrature. For frequencies other than 10 MHz, see [31].

- Change in operating conditions between the beat note and noise measurement.
- Accuracy of the noise measurement.
- Spectrum analyzer amplitude accuracy, measurement error tends to increase at very low levels or there may be dynamic range limitations.
- Noise bandwidth correction.
- Detector corrections.
- Noise contribution of reference oscillator.
- External interference, particularly line frequency related spurious.
- Hardware issues.
- Inadequate isolation, injection locking.
- Mixer offset/offset phase error.
- Gain accuracy.
- PLL response peaking (described below).
- Noise contribution of LNA.

The potential errors should not be a deterrent to making phase noise measurements. Knowledge of where the errors are can aid in designing to mitigate them and in choosing system components. A comprehensive analysis of errors can be found in **[32]**.

The largest errors are probably those associated with the actual level measurements and potential external interference. Consistent measurements with less than 2 to 4 dB variation were routinely obtained and that should be adequate for most amateur applications.

The two phase noise measurement techniques described here are probably the ones most useful to amateurs but there are others **[33]**. There are digital solutions such as the R&S FSWP described above that offer better performance but they are more

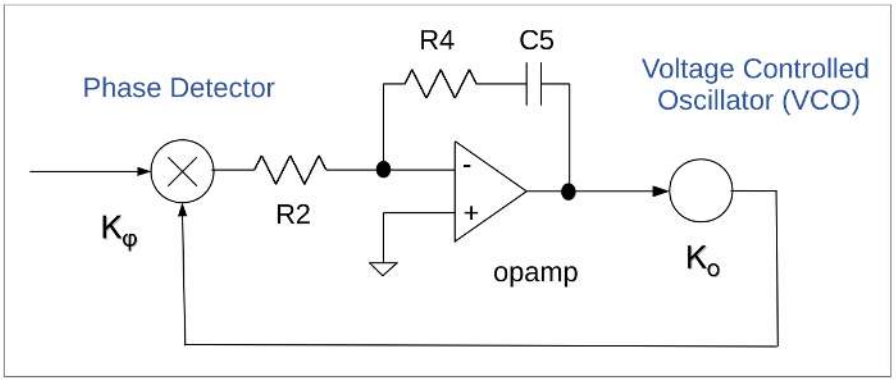

Figure 15 — PLL loop filter circuit in Figure 8.

complex (and expensive!). The concept behind the digital analysis is briefly described in **[2]**. The PLL phase noise measurement system described here is based on classic analog techniques, and many of the parts necessary to implement it may already reside on your workbench or in your junk box.

Appendix I: Phase Locked Loop Analysis

A simple type 2 second order loop is adequate for the PLL **[34]**. **Figure 15** is the PLL circuit from the phase noise box.

Two Bliley NV26R891 100 MHz OCXOs were used in the example above. Their tuning sensitivity, K_o was measured as 181 Hz/V. This measurement was done by recording the voltage needed to offset the NV26R891 ±200 Hz at 100 MHz. The phase detector sensitivity K_φ was available from the phase detector calibration measurement. The peak voltage of the beat frequency signal provides:

$$K_\varphi = \sqrt{2}\left(10^{(V_{brms}/20)}\right) = \left(\sqrt{2}\cdot 0.110\right)$$
$$= 0.156 \text{ V/rad}$$

which is −19.14 dB.

$$K = K_o K_\varphi = (2\pi)(181)(0.156) = 177.4$$

Calculate the loop natural frequency ω_n. For the loop filter, choose a large-value low-leakage capacitor. This reduces the value of the resistor in the integrator. Lower values produce a lower level of resistor noise. Electrolytic and tantalum capacitors are polarized and probably have too much leakage. Use a ceramic or plastic film capacitor. Such capacitors are available in the 1 – 10 µF range. A 2.2 µF ceramic capacitor was used.

$$\omega_n = \sqrt{\frac{K}{R_2 C_5}} = \sqrt{\frac{177.4}{(100\text{ k})(2.2\ \mu\text{F})}}$$
$$= 28.4 \text{ rad/sec} = 4.52 \text{ Hz}$$

Next set the damping factor ζ. While smaller values improve loop transient response, they produce an undesirable peaking in the loop response around ω_n. This peaking can bias noise measurements that approach the loop bandwidth. Values of 1.5 to 2.0 produce a flatter response but they tend to increase the loop bandwidth.

$$\zeta = \frac{\tau_2}{2}\omega_n = \frac{(C_5)(R_4)}{2}\omega_n$$
$$= \frac{(2.2\ \Omega\ \text{F})(51{,}000\ \Omega)}{2}(28.4) = 1.59\ .$$

With ω_n and ζ, calculate the loop 3 dB bandwidth. This bandwidth should be 1/10th the lowest offset frequency.

$$\text{BW}_{3\text{dB}} = \omega_n\sqrt{\left(2\zeta^2+1+\sqrt{\left(2\zeta^2+1\right)^2+1}\right)}$$
$$= 99.2 \text{ rad/sec} = 15.8 \text{ Hz.}$$

Measurement down to about 200 Hz offset from the carrier, maybe even down to 100 Hz, is possible with this PLL. If the choices for R2/C5 don't give the desired bandwidth, pick a new R2 and/or C5 and start again. A spreadsheet program was written to calculate loop parameters.

Dennis Sweeney, WA4LPR, was first licensed as a Novice, WN4LPR, in 1963, and subsequently upgraded to Technician, Advanced, and now Amateur Extra class. He is retired from the faculty of VA Tech in Blacksburg, VA as manager of the undergraduate lab program for VA Tech's Electrical and Computer Engineering Department. He taught electronics, satellite communications and radio engineering. He also worked with satellite systems for the Aerospace Corporation. Dennis holds a PhD in Electrical Engineering and is a Senior Member of the IEEE. He is active on 6 m, 70 cm, 23 cm and 3 cm, much with home brew equipment. He really enjoys building things. Dennis is one of the founding members of the Blue Ridge Microwave Society.

References

[1] Keysight Technologies, "Phase Noise 101 Basics, Applications and Measurements," 2019, pp. 12-14.

[2] **https://www.youtube.com/watch?v=hfgaEjf1154**

[3] HP application note AN 283-3, "Low Phase Noise Applications of the HP8662A and 8663A Synthesized Signal Generators," December 1986. See [15] for a copy.

[4] Hewlett-Packard RF and Phase Noise Measurement Seminar, June 1985. See [15] for a copy.

[5] B. E. Pontius, NØADL, "Measurement of Signal-Source Phase Noise with Low-Cost Equipment," *QEX*, No. 188, May/June 1998, pp. 38-49.

[6] J. F. M. Van der List, PAØJOZ, "Experiments with Phase-Noise Measurement," *QEX*, No. 192, Jan./Feb. 1999, pp. 31-41.

[7] Kjell Karlsen, LA2NI, "A Method of Measuring Phase Noise in Oscillators," *QEX*, No. 227, Nov./Dec. 2004, pp 54 - 59.

[8] Jacob Makhinson, N6NWP, "DEMPHANO," Communications Quarterly, Vol. 9, No. 2, Spring 1999, pp. 9-17. This paper is included on the CD anthology provided with Hayward, Campbell, and Larkin, "Experimental Methods in RF Design," *ARRL*, 2003.

[9] John Miles, KE5FX, "Frequency Stability Measurement: Technologies, Trends, and Tricks," *Microwave Update 2010*, Cerritos, CA, October 21-24, 2010, pp. 116-133.

[10] Hans Wagemans, ON4CDU, and Christopher Huygen, ON4IY, "Agile Sources based on the ADF5355 Microwave Wideband Synthesizer with Integrated VCO," *DUBUS*, Vol. 50, 1/2021, pp. 71-85.

[11] Dennis Sweeney, WA4LPR, "The Science and Practice of Phase Noise Measurement," *Microwave Update 2011*, Enfield, CT, Oct. 13-16, 2011, pp. 13-37.

[12] Bruce E. Pontius, NØADL, "Measurement of Signal-Source Phase Noise with Low-Cost Equipment," op. cit.

[13] Kjell Karlsen, LA2NI, "A Method of Measuring Phase Noise in Oscillators," op. cit.

[14] **http://prologix.biz/**

[15] **http://www.thegleam.com/ke5fx/**

[16] **https://www.quanticwenzel.com/** (search on "phase noise"); **https://wenzel22.wpenginepowered.com/wp-content/uploads/BP_1000_v1-05.pdf**; **http://techlib.com/files/lowamp.pdf**; see also [15].

17] Mini-Circuits, "Frequently asked questions about phase detectors," AN-41-001, 2015, pp 1-7. See: **https://www.minicircuits.com/appdoc/AN41-001.html**.

[18] Stephen R. Kurtz, "Mixers as Phase Detectors," *WJ Technote*, Vol. 5 No.1, Jan./Feb. 1978, revised 2001. See: **https://www.rfcafe.com/references/articles/wj-tech-notes/Mixers_phase_detectors.pdf**.

[19] Hewlett Packard, "Residual Phase Noise and AM Noise Measurement Techniques," 1990, Chapter 2.

[20] Mini-Circuits, AN-41-001, op. cit.

[21] Agilent Technologies, "Phase Noise Characterization of Microwave Oscillators: Phase Detector Method," Product Note 11729B-1, 2007, p. 29. Source noise correction.

[22] HP AN_283-3, op. cit., Appendix A: Calculation of Phase Noise of Three Unknown Sources.

[23] Warren Walls, "Practical Problems Involving Phase Noise Measurement," 33rd Annual Precise Time and Time Interval (PTTI) Meeting, 2001, pp 407 – 416. See: **https://apps.dtic.mil/sti/pdfs/ADA485797.pdf**.

[24] Jacob Makhinson, N6NWP, "DEMPHANO," op. ct.

[25] **https://digilent.com/reference/test-and-measurement/analog-discovery-2/start**.

[26] J. F. M. Van der List, PAØJOZ, "Experiments with Phase-Noise Measurement," op. cit.

[27] Arthur B. William, and Fred J. Taylor, *Electronic Filter Design Handbook*, McGraw-Hill, New York, 2nd ed, 1988, ISBN 0-07-070434-1, Section 5.2.

[28] Jim Williams and Todd Owen, "Understanding and selecting rms voltmeters," *Electronic Design News* (EDN) , May 11, 2000, pp. 54-58.

[29] Paul Horowitz and Winfield Hill, *The Art of Electronics,* Third Edition, Cambridge University Press, 2015, ISBN 978-0-521-80926-9, Section 8.9.

[30] **http://www.dicks-website.eu/noisecalculator/index.html.**

[31] Reed Fisher, W2CQH, "Twisted-Wire Quadrature Hybrid Directional Couplers," *QST*, Jan. 1978, pp. 21-23. Included on the CD anthology provided with Hayward, Campbell, and Larkin, *Experimental Methods in RF Design, ARRL*, 2003.

[32] Agilent Product Note 11729B-1, "Phase Noise Characterization of Microwave Oscillators: Phase Detector Method," op. cit.

[33] Ulrich L. Rohde and Ajay K. Poddar, "Getting Its Measure," *IEEE Microwave Magazine,* Sep./ Oct. 2013, pp. 73-86.

[34] Floyd M. Gardener, *Phaselock Techniques*, John Wiley & Sons, New York, 1996, Chapter 1.

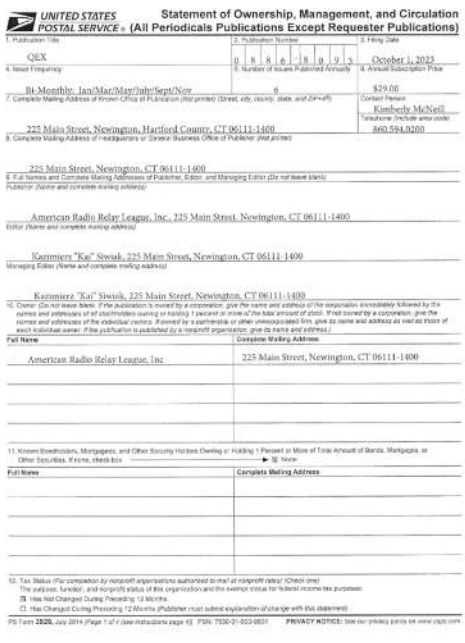

UNITED STATES POSTAL SERVICE® Statement of Ownership, Management, and Circulation (All Periodicals Publications Except Requester Publications)

1. Publication Title: QEX
2. Publication Number: 0 8 8 6 - 1 8 0 9 3
3. Filing Date: October 1, 2023
4. Issue Frequency: Bi-Monthly: Jan/Mar/May/July/Sept/Nov
5. Number of Issues Published Annually: 6
6. Annual Subscription Price: $29.00
7. Complete Mailing Address of Known Office of Publication (Not printer) (Street, city, county, state, and ZIP+4®): 225 Main Street, Newington, Hartford County, CT 06111-1400
Contact Person: Kimberly McNeill
Telephone (Include area code): 860.594.0200
8. Complete Mailing Address of Headquarters or General Business Office of Publisher (Not printer): 225 Main Street, Newington, CT 06111-1400
9. Full Names and Complete Mailing Addresses of Publisher, Editor, and Managing Editor (Do not leave blank)
Publisher (Name and complete mailing address): American Radio Relay League, Inc, 225 Main Street, Newington, CT 06111-1400
Editor (Name and complete mailing address): Kazimierz "Kai" Siwiak, 225 Main Street, Newington, CT 06111-1400
Managing Editor (Name and complete mailing address): Kazimierz "Kai" Siwiak, 225 Main Street, Newington, CT 06111-1400
10. Owner (Do not leave blank. If the publication is owned by a corporation, give the name and address of the corporation immediately followed by the names and addresses of all stockholders owning or holding 1 percent or more of the total amount of stock. If not owned by a corporation, give the names and addresses of the individual owners. If owned by a partnership or other unincorporated firm, give its name and address as well as those of each individual owner. If the publication is published by a nonprofit organization, give its name and address.)

Full Name	Complete Mailing Address
American Radio Relay League, Inc	225 Main Street, Newington, CT 06111-1400

11. Known Bondholders, Mortgagees, and Other Security Holders Owning or Holding 1 Percent or More of Total Amount of Bonds, Mortgages, or Other Securities. If none, check box → ☒ None

Full Name	Complete Mailing Address

12. Tax Status (For completion by nonprofit organizations authorized to mail at nonprofit rates) (Check one)
The purpose, function, and nonprofit status of this organization and the exempt status for federal income tax purposes:
☒ Has Not Changed During Preceding 12 Months
☐ Has Changed During Preceding 12 Months (Publisher must submit explanation of change with this statement)

PS Form 3526, July 2014 (Page 1 of 4 (see instructions page 4)) PSN: 7530-01-000-9931 PRIVACY NOTICE: See our privacy policy on www.usps.com

13. Publication Title: QEX
14. Issue Date for Circulation Data Below: Sept/Oct 22-July/Aug 23 | Sept/Oct 2023

15. Extent and Nature of Circulation			Average No. Copies Each Issue During Preceding 12 Months	No. Copies of Single Issue Published Nearest to Filing Date
a. Total Number of Copies (Net press run)			4808	3600
b. Paid Circulation (By Mail and Outside the Mail)	(1)	Mailed Outside-County Paid Subscriptions Stated on PS Form 3541 (Include paid distribution above nominal rate, advertiser's proof copies, and exchange copies)	3439	2936
	(2)	Mailed In-County Paid Subscriptions Stated on PS Form 3541 (Include paid distribution above nominal rate, advertiser's proof copies, and exchange copies)	0	0
	(3)	Paid Distribution Outside the Mails Including Sales Through Dealers and Carriers, Street Vendors, Counter Sales, and Other Paid Distribution Outside USPS®	355	444
	(4)	Paid Distribution by Other Classes of Mail Through the USPS (e.g., First-Class Mail®)	437	343
c. Total Paid Distribution (Sum of 15b (1), (2), (3), and (4))			3831	3423
d. Free or Nominal Rate Distribution (By Mail and Outside the Mail)	(1)	Free or Nominal Rate Outside-County Copies included on PS Form 3541	50	50
	(2)	Free or Nominal Rate In-County Copies included on PS Form 3541	0	0
	(3)	Free or Nominal Rate Copies Mailed at Other Classes Through the USPS (e.g., First-Class Mail)	73	83
	(4)	Free or Nominal Rate Distribution Outside the Mail (Carriers or other means)	82	82
e. Total Free or Nominal Rate Distribution (Sum of 15d (1), (2), (3) and (4))			206	215
f. Total Distribution (Sum of 15c and 15e)			4037	3641
g. Copies not Distributed (See Instructions to Publishers #4 (page #3))			1191	1059
h. Total (Sum of 15f and g)			4838	3900
i. Percent Paid (15c divided by 15f times 100)			94.90%	92.40%

If you are claiming electronic copies, go to line 16 on page 3. If you are not claiming electronic copies, skip to line 17 on page 3.

PS Form 3526, July 2014 (Page 2 of 4)

UNITED STATES POSTAL SERVICE® Statement of Ownership, Management, and Circulation (All Periodicals Publications Except Requester Publications)

16. Electronic Copy Circulation

	Average No. Copies Each Issue During Preceding 12 Months	No. Copies of Single Issue Published Nearest to Filing Date
N/A		
a. Paid Electronic Copies		
b. Total Paid Print Copies (Line 15c) + Paid Electronic Copies (Line 16a)		
c. Total Print Distribution (Line 15f) + Paid Electronic Copies (Line 16a)		
d. Percent Paid (Both Print & Electronic Copies) (16b divided by 16c × 100)		

☒ I certify that 50% of all my distributed copies (electronic and print) are paid above a nominal price.

17. Publication of Statement of Ownership
☒ If the publication is a general publication, publication of this statement is required. Will be printed in the January/February 2024 issue of this publication. ☐ Publication not required

18. Signature and Title of Editor, Publisher, Business Manager, or Owner: Kai Siwiak, CFO — Date: 9/29/23

I certify that all information furnished on this form is true and complete. I understand that anyone who furnishes false or misleading information on this form or who omits material or information requested on the form may be subject to criminal sanctions (including fines and imprisonment) and/or civil sanctions (including civil penalties).

PS Form 3526, July 2014 (Page 3 of 4) PRIVACY NOTICE: See our privacy policy on www.usps.com

Eric P. Nichols, KL7AJ
138 Shenandoah Drive, Fairbanks, AK 99712 | **kl7aj@arrl.net**

Self-Paced Essays – #19
The Smith Chart, Plain and Fancy

The Smith Chart is an easy way of performing transmission line calculations.

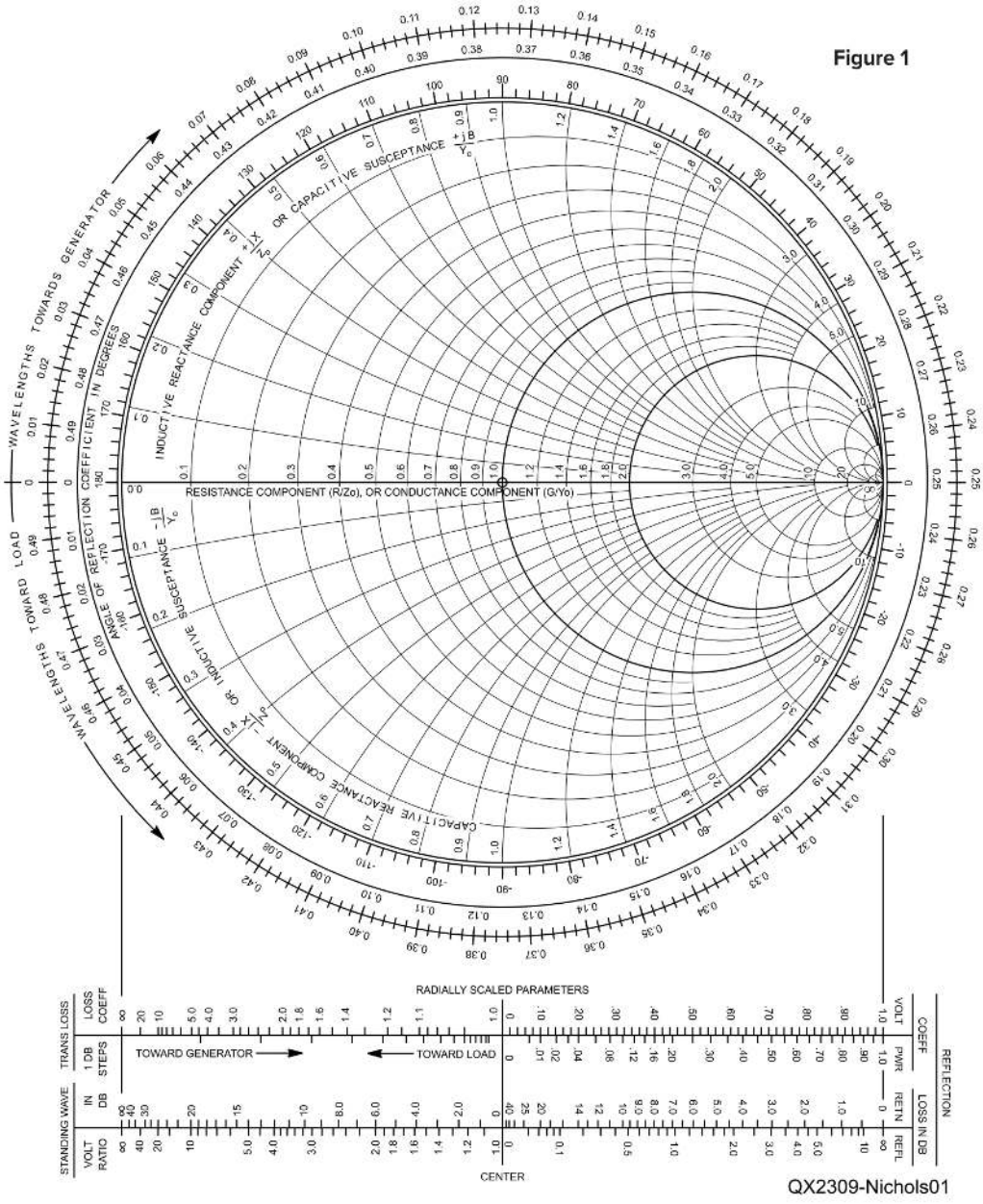

Figure 1

QX2309-Nichols01

In our previous *Essay*, we introduced the Vector Network Analyzer, an instrument so handy and inexpensive that there's really no excuse for any ham or electronics experimenter not to have one. My new NanoVNA just arrived yesterday; I had sold a slightly older version to a new ham who was very excited to play with this new technology. However, in keeping with my philosophy that it's always best to know the answer before you hand it over to a computer, we're first going to discuss the "hard way" of doing things with the Smith Chart, which is itself a major simplification of the "real hard way" of performing transmission line calculations.

To really appreciate the Smith Chart, let us first look at the equation (19) from which the Smith Chart was derived, see the 24th edition of the *ARRL Antenna Book*; here reproduced as **Eqn (1)**:

$$Z_{in} = Z_0 \frac{Z_L \cosh(\gamma l) + Z_0 \sinh(\gamma l)}{Z_L \sinh(\gamma l) + Z_0 \cosh(\gamma l)}$$

where:
Z_{in} = complex impedance at input of line
Z_L = complex impedance at end of line = $R_a \pm jX_a$
Z_0 = characteristic impedance of line = $R_0 - jX_0$
l = physical length of line
$\gamma = \alpha + j\,\beta$
α = matched loss attenuation constant in nepers/unit length-line (1 neper = 8.686 dB)
β = phase constant of line in radians/unit length, where 2π radians = one wavelength
and where:

$$\beta = \frac{2\pi}{VF \times 983.6 / f_{MHz}} \text{ for } l \text{ in feet}$$

VF = velocity factor.

Whenever my students complain about how hard the Smith Chart is, I simply refer them to the equations above and ask them if they want to do it this way. The Smith Chart always wins.

Now, in the previous *Essay*, we pointed out that the typical VNA is normalized to 50 Ω, since that is the characteristic impedance of the most common coaxial transmission line. The "full-fledged" Smith Chart, **Figure 1**, is non-normalized, which means you can use it with any impedance transmission line, with a couple of extra steps involved. The *ARRL Antenna Book* also has some high resolution charts you can work with in the chapter on transmission lines. Things can get a little "cramped" on the "adult version" of the Smith Chart.

Let's take a simple example of a quarter-wave length of 600 Ω ladder line, with a load consisting of a 50 Ω resistor and a 50 Ω inductor in series. Our task is to find out what the input impedance of the transmission line is. Using classic "*j* notation" our load impedance is (50 + *j* 50) Ω. The *j* is positive because it is inductive. First we need to normalize the impedance, which means we divide each term (the resistance and reactance) separately by the characteristic impedance of the line. In this case our normalized impedance is 50/600 +*j* 50/600, or 0.083 + *j* 0.083. Unless you use a really fine point on your pencil, you probably will not be able to resolve more than two significant digits. In fact, for this example, we'll use just (0.08 + *j* 0.08) Ω. That point is plotted near the left extreme of the chart of **Figure 2**.

Now, before we go any further, let's do one optional step that will really reveal a lot about this whole matter. Locate a compass (the circle making kind). Stick the pointy part of the compass

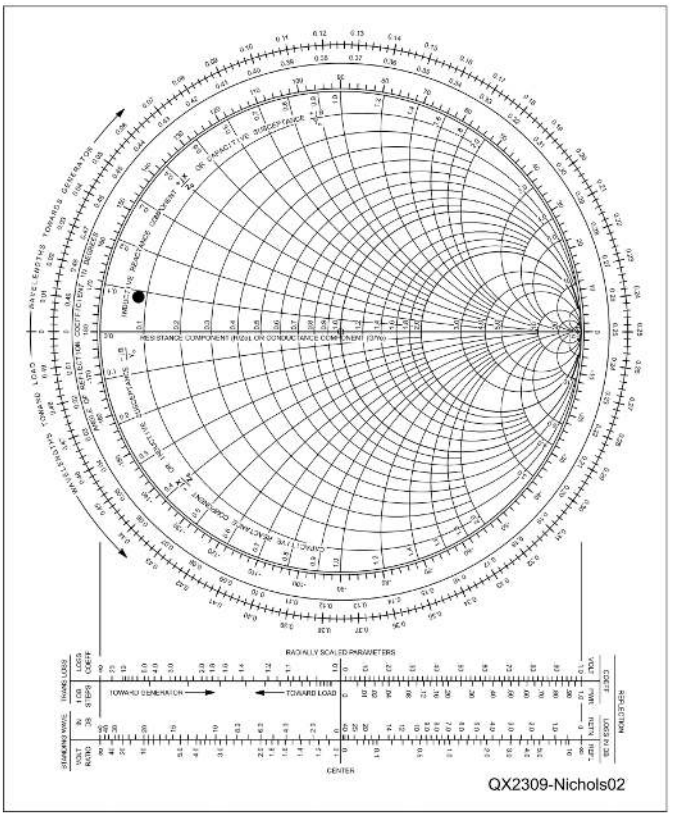

Figure 2

dead center of the chart (the origin), and place the pencil on the impedance point you plotted above. Now draw a complete circle around the chart, see **Figure 3**.

The circle you've just drawn is the SWR circle, which is the *locus* of every possible impedance that can exist on this particular transmission line. If you were to drop a line segment down from the very left extreme of the SWR circle (where it crosses the horizontal axis) on down to the "radial scaled parameters," you will be able to read the SWR directly, in this case, just a smidgen above 12:1 SWR. If there were no reactance in the load, the SWR would be *exactly* 12:1.

Now, let's take a straight edge, and draw a line segment from our original point, through the origin, and on through to where it intersects with the SWR circle on the "southeast" side (**Figure 4**).

The point of intersection is our new impedance, which is *about* 13 – *j* 5.0 ohms. Why the negative *j*? Because we are now below the "horizon," where all values are capacitive. But we still have one more step to perform. We need to *de-normalize* our impedance, which means we need to *multiply* each term by the characteristic impedance. This gives us 13×600 – *j* 5.0×600, or 7800 – *j* 3000 ohms, which is our input impedance.

This impedance isn't likely to make many transmitters happy. However, if we add *another* quarter wave of transmission line, this will bring our impedance right back to where we started, which is 50 + *j* 50 ohms, which isn't too bad a mismatch. For a typical 50 ohm transmitter, this will look like about a 2.5:1 SWR, not great, but usable.

You can, of course, use this method for any length of transmission line, using the wavelengths toward generator or wave-

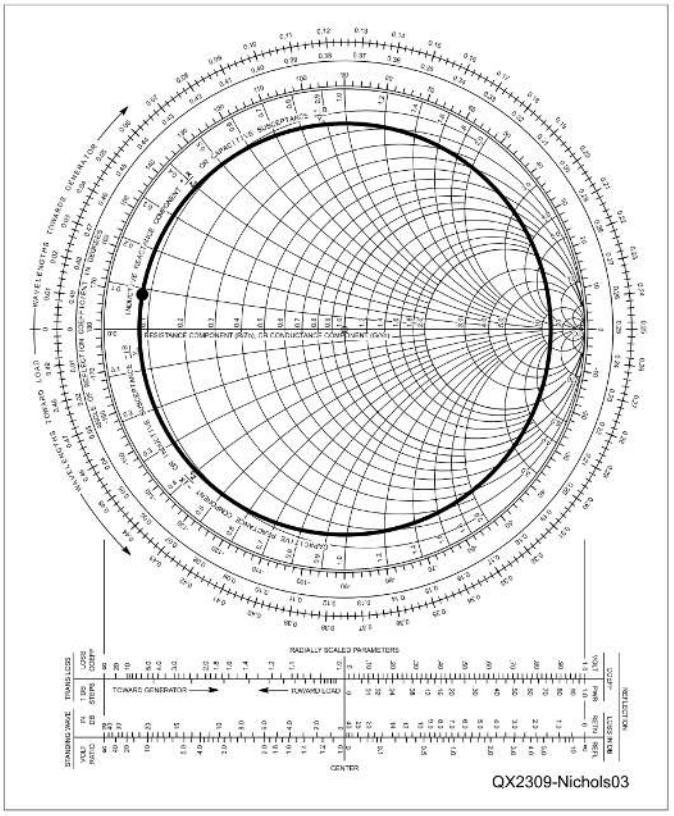

Figure 3

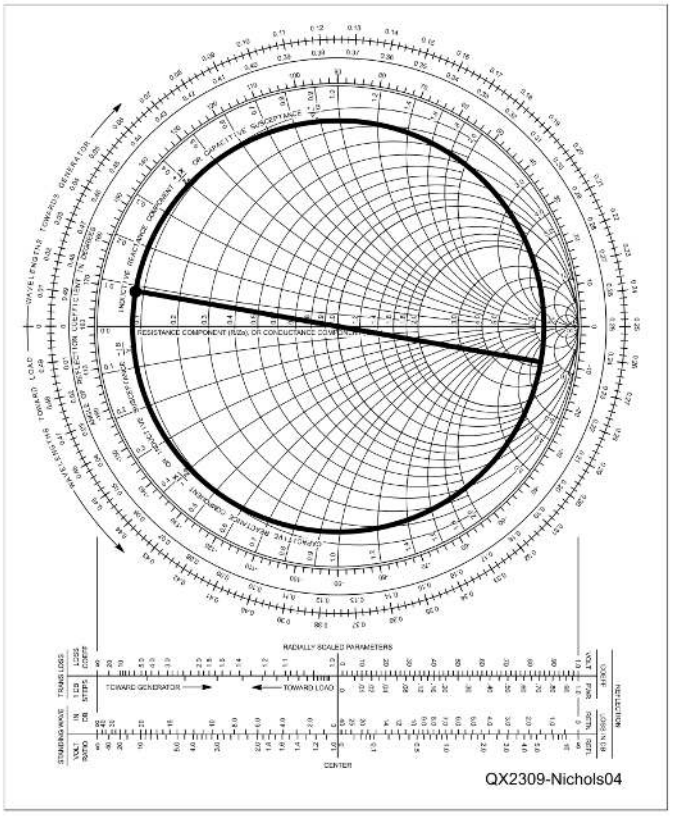

Figure 4

lengths toward load scales on the outer perimeter of the chart. Quarter wave increments are just simpler to follow, because you just go diametrically across the chart. Remember than any possible impedance will lie somewhere on your SWR circle. By the way, it is always best to convert frequencies to wavelengths first, before doing any Smith Chart calculations.

After a few transmission line calculations, the Smith Chart will become second nature. Really! Now with the ready availability of the NanoVNA, you can check your work very quickly.

Here are a few "self-evident truths" that the Smith Chart clearly presents, which can greatly increase your grasp of transmission lines.

1) The greater the SWR, the greater will be the radius of the SWR circle. From a practical standpoint, this means that the greater the SWR, the greater the *variation* of impedance as you move along the transmission line. A "flat" transmission line will simply be a point in the center of the Smith Chart.
2) Impedances change much more rapidly with respect to frequency near the right hand side of the Smith Chart. This graphically explains the "squirrely" behavior of high impedance antennas like the increasingly popular End Fed Half Wave (EFHW) antenna.
3) A purely reactive load will fall on the outer perimeter of the Smith Chart, meaning that with no resistance in the load, the SWR will always be infinite.

As always, we invite your comments and questions; we want to keep these *Essays* as interactive as possible. If we need to camp out a little longer on any particular topic, we can do that. Usually, the Smith Chart merits a few passes, as it is not only important, but fairly complicated to many folks. It is well worth understanding *completely.*

Next essay, we will talk a bit about antenna modeling, and the merits of verifying your antenna models with real world physical construction. — *73, until next time, Eric.*

Upgrade Your Station's Performance with DX Engineering!

Noise Cancellation and Audio Enhancement Products

bhi Noise Cancellation Products

By harnessing cutting-edge digital signal processing technology, bhi noise cancellation and audio enhancement products make it easier for you to discern weak audio signals and increase your radio listening enjoyment. Choose from DSP and extension speakers, DSP devices, and the ParaPro EQ20 Parametric Equalizer, which allows you to adjust any part of the frequency range to customize receive audio to suit your own hearing. **Enter "bhi" at DXEngineering.com. Speakers from $35.99; noise-cancelling modules from $235.99**

Hamplus

HAMPLUS

Hamplus makes innovative RF and control switching components tailored to the amateur radio community. The Hamplus line includes rotator switches, smart control consoles, and antenna switches that can read data from the radio and memorize antenna selections. DX and contest stations worldwide depend on Hamplus for proven results. In an exclusive arrangement, North American operators can enjoy the same advantage by ordering Hamplus products through DX Engineering. **Enter "Hamplus" at DXEngineering.com. Antenna switches from $259.99**

DX ENGINEERING

DX Engineering Receiving Equipment

Choose from unique receiving gear from the hams at DX Engineering, including the NCC-2 Receive Antenna Phasing System; RTR-2 Modular Receive-Transmit Interface for safely adding a receive antenna to a transceiver; DMC-2 Dual Module Chassis for plugging in filters and receiver protection devices; 2-Port Splitter/Combiners that split one RF signal to feed two receivers; and the Receiver Guard Electronic RF Limiter. **Enter "DXE Receiving" at DXEngineering.com.**

HF Amplifiers

ACOM Outstanding HF Power Products

ACOM has built a reputation among HF contesters and DX chasers for its outstanding RF power amplifiers, including the 700S HF+6, featuring 700 watts of output power (PEP SSB or CW); the solid state 1200S 1,000 Watt HF+6, with 5" high-resolution color display; and 2100, which boasts 1,500 watts PEP and virtually-silent QSK. **Enter "ACOM" at DXEngineering.com. From $2,659.99**

GEOCHRON

Digital Atlas 2 4K

Geochron's Digital Atlas 2 4K gives viewers magnificent displays of the Earth with sunrise-sunset rendered in real time through a small computer that plugs directly into a 4K TV (not provided) via HDMI. Ham-friendly features include a Grey Line display; DX prefixes; and month, day, and hour of every time zone, including Zulu Time. Version II (GEO-400-1000B) comes with faster refresh rates, global weather overlays, live location of the International Space Station, and more. **Enter "Digital Atlas" at DXEngineering.com. $449.00**

DX ENGINEERING

Transceiver Key Line Splitters and Combiners

Choose from three passive DC-only devices for the "ground-on-transmit" amplifier keying line of one or multiple transceivers. These splitters/combiners are handy when using amateur radio devices that need to "share" a T/R keying line and don't have a keying line pass-through. The DXE-KEYLINE-3 is a splitter for one transceiver to key one amp and two accessories; the DXE-3RIGKEYLINE is a combiner for up to three transceivers to key one amp; and the DXE-KEYLINE-DUAL is a combiner-splitter for two transceivers to key two amps, or one amp and one accessory. **Enter "DXE Key Diode" at DXEngineering.com. From $73.99**

DX ENGINEERING

PRO-STACK Broadband Antenna Phasing Systems

These systems deliver broadband coverage on 160-10M, boast power handling up to 5kW, and allow you to combine multiple Yagi, log periodic, beam, or quarter-wave verticals for enhanced directional pattern selections and dramatically improved HF operations. The PRO-STACK switch relay and control console combo allows multiple selections of any or all antennas including in and out of phase combinations. There are two- and three-antenna systems available with SO-239, Type N, or 7-16 DIN connectors. **Enter "Pro-Stack" at DXEngineering.com. From $709.98**

YAESU ICOM KENWOOD ALINCO WiMO InnoAntennas OPTIBEAM EA

Read What's New in Ham Radio at Our Blog, OnAllBands.com!

DX ENGINEERING®

Ordering (via phone) Country Code: +1
9 am to midnight ET, Monday-Friday
9 am to 5 pm ET, Weekends
Phone or e-mail Tech Support: 330-572-3200
9 am to 7 pm ET, Monday-Friday
9 am to 5 pm ET, Saturday
Email: DXEngineering@DXEngineering.com

Ohio Showroom Hours:
9 am to 5 pm ET, Monday-Saturday
Ohio Curbside Pickup:
9 am to 8 pm ET, Monday-Saturday
9 am to 7 pm ET, Sunday
Nevada Curbside Pickup:
9 am to 7 pm PT, Monday-Sunday

800-777-0703 | DXEngineering.com

ON ALL BANDS

Email Support 24/7/365 at DXEngineering@DXEngineering.com

Prices subject to change without notice. Please check DXEngineering.com for current pricing.

Holiday Cheers
For Your Favorite Ham

*Optional
CX-10G
10GHz Transverter

IC-905
2M / 70CM / 23CM / 13CM / 5CM

IC-T10
2M / 70CM Analog

ID-50A
2M / 70CM
Analog / Digital

ID-52A
2M / 70CM
Analog / Digital

IC-705
HF / 6M / 2M / 70CM

Shipping Now

IC-7300
HF / 6M

IC-7100
HF / 6M / 2M / 70CM Analog / Digital

ID-5100AD
2M / 70CM Analog / Digital

IC-7610
HF / 6M

IC-V3500
2M Analog

For the love of **ham radio.**

www.icomamerica.com/amateur
insidesales@icomamerica.com

ICOM®